

STEIN VARIATIONAL GRADIENT DESCENT ON INFINITE-DIMENSIONAL SPACE AND APPLICATIONS TO STATISTICAL INVERSE PROBLEMS

JUNXIONG JIA AND DEYU MENG

ABSTRACT. For solving Bayesian inverse problems governed by large-scale forward problems, we present an infinite-dimensional version of the Stein variational gradient descent (iSVGd) method, which has the ability to generate approximate samples from the posteriors efficiently. Specifically, we introduce the concept of the operator-valued kernel and the corresponding function-valued reproducing kernel Hilbert space (RKHS). Through the properties of RKHS, we give an explicit meaning of the infinite-dimensional objects (e.g., the Stein operator) and prove that the infinite-dimensional objects are indeed the limit of finite-dimensional items. Furthermore, by generalizing the change of variables formula, we construct iSVGd with preconditioning operators, yielding more efficient iSVGd. During these generalizations, we introduce a regularity parameter $s \in [0, 1]$. Our analysis shows that the intuitive trivial version (i.e., by directly taking finite-dimensional objects as infinite-dimensional items) of iSVGd with preconditioning operators ($s = 0$) will yield inaccurate estimates, and the parameter s should be chosen larger than 0 and smaller than 0.5. Finally, the proposed algorithms are applied to an inverse problem governed by the Helmholtz equation. Numerical results confirm the correctness of our theoretical findings and demonstrate the potential usefulness of the proposed approach in the posterior sampling of large-scale nonlinear statistical inverse problems.

1. INTRODUCTION

The Bayesian approach to inverse problems has grown in popularity significantly over the last decade, driven by recent algorithmic innovation and steadily increasing computer power. By transforming the inverse problems into statistical inference problems, the Bayesian approach provides a general framework for quantifying uncertainties of inverse problems [1]. The posterior distribution automatically delivers an estimate of the statistical uncertainty in the reconstruction, and hence suggests “confidence” intervals that allow to reject or accept scientific hypotheses [37], which is useful for practical applications, e.g., artifact detecting in medical imaging [53].

For applying the Bayesian approach, the appropriate Bayes’ model is needed to be established firstly. When the inferred parameters are in a finite-dimensional space, the finite-dimensional Bayesian method can be employed, as is explored firstly in the geophysics community since 1982 [47]. Specially, a nice survey on such finite-dimensional theory has been provided by Kaipio and Somersalo in 2005 [30]. However, when the inferred parameters are in the infinite-dimensional space, the

2010 *Mathematics Subject Classification.* 65L09, 49N45, 62F15.

Key words and phrases. inverse problems, variational inference method, Stein variational gradient descent, Helmholtz equation, machine learning.

problems are more difficult to tackle since the Lebesgue measure cannot be strictly defined in this case [15]. Some attempts have been made against this difficulty recently. For example, in 2009, Cotter et al. [13] designed a general well-posedness framework for Bayesian formula and applied the general theory to inverse problems of fluid mechanic equations. Besides, Stuart presented a long survey [44], which illustrates the basic framework for using infinite-dimensional Bayes' approach to inverse problems. Since inverse problems of partial differential equations (PDEs) often meet function parameters that belong to some infinite-dimensional space, the infinite-dimensional Bayes' theory has gradually attracted more attention in the recent decade [5, 12, 22, 39, 40].

As discussed in [1], many of the challenges in Bayesian inverse approach are associated with how to effectively extract information encoded underlying the posterior probability measure. Currently, there are two main strategies, namely, the point estimate method and the sampling method. For the point estimate method, finding the maximum a posteriori (MAP) estimate is equivalently reformulated as solving an optimization problem [5, 22]. In some situations, MAP estimates are more desirable and computational feasible than the entire posterior distribution [24, 46]. However, point estimates cannot transmit uncertainty information and are usually recognized as incomplete Bayes' method.

Sampling type methods, such as the well known Markov chain Monte Carlo (MCMC), are often used to extract posterior information. Sampling type methods in the finite-dimensional setting are well studied, and we refer the interested reader to [31] for more introductions. Although the MCMC methods designed for finite-dimensional problems are accurate and effective, they are usually not robust under mesh refinement. Against this issue, Cotter et al. [12] proposed the MCMC method defined on function space in 2013, which is robust under mesh refinement. Later on, multiple dimension-independent MCMC-type algorithms have been presented [14, 19, 43]. These MCMC-type algorithms, however, still need unaffordable computational cost, making them hardly available in many applications, e.g., seismic exploration [20].

For finite-dimensional problems, there are many investigations focused on seeking algorithms with both uncertainty quantification capability and computational efficiency. Especially in machine learning, variational inference (VI) methods have been broadly investigated that can ameliorate both above two issues [2, 36, 51, 52]. The early attempt is made for finite-dimensional inverse problems. Under the mean-field assumptions, Jin et al. [28, 27] investigated linear problems under a hierarchical formulation with Gaussian and centered-t noise distribution. Then, Guhua et al. [21] considered skewed-t noise distribution under a similar setting. In 2016, Liu and Wang [32] proposed a new type of variational inference algorithm named the Stein variational gradient descent (SVGD), which achieves reliable uncertainty estimation using an interacting repulsive mechanism in an efficient manner. In various challenging machine learning problems, SVGD has shown to be a fast and flexible algorithm. Such an efficient method has also been involved into solving the inverse problems of PDEs. Particularly, Chen et al. [10, 11] proposed projected Stein variational Newton method and Stein variational reduced basis method. Their investigations validate that SVGD can solve inverse problems of PDEs efficiently and give reliable uncertainty estimation.

For infinite-dimensional problems, the research on the variational inference (VI) is still in its infancy. When the approximate measures are restricted to be Gaussian, Pinski et al. [39, 40] employed a calculus-of-variations viewpoint to investigate the VI method and developed a novel algorithm based on the Robbins-Monro algorithm. Sun et al. [45] proved that the Kullback-Leibler (KL) divergence between the stochastic processes is equal to the supremum of the KL divergence between the measures restricted to finite marginals. And they developed a VI method for functions parameterized by Bayesian neural networks. Under the classical mean-field assumption, Jia et al. [26] recently proposed a general VI framework defined on separable Hilbert space. Concerned with the SVGD, Wang et al. [50] proposed a function space particle optimization method that solve the particle optimization directly in the space of functions. Later on, this function space algorithm has been employed to solve computer vision tasks [9], e.g., the context of semantic segmentation and depth estimation. However, the current investigations on the function spaced SVGD require to assume that the random functions are able to be parameterized by a finite number of parameters, e.g., parameterized by some neural network [50]. Hence, the probability measures on functions are implicitly defined through the probability distributions of finite-number of parameters, while not directly on the expected infinite-dimensional function space.

In this study, we focus on inverse problems of PDEs imposed on infinite dimensional function space directly instead of training neural networks. Specifically, following the spirit of investigations on the preconditioned Crank-Nicolson (pCN) algorithm [12], we aim to construct SVGD on separable Hilbert space with random functions, i.e., directly on infinite-dimensional function space, instead of approximately parameterized by a fixed finite number of parameters. In the following, for conciseness, we use iSVGD stands for SVGD defined on the infinite-dimensional function space. Our main focus is to obtain algorithms defined on Hilbert space through this construction, which are the foundations for performing appropriate discretizations. With the well-defined infinite-dimensional algorithms, performing rigorous numerical analysis (e.g., convergence of the algorithms) is possible for inverse problems of PDEs under nonparametric setting. The contribution of our work can be summarized as follows:

- Considering the Bayesian formula in infinite-dimensional space, we provide the rigorous meaning of the SVGD on the separable Hilbert space, called iSVGD. We define the Stein operator and the corresponding optimization problem on some Hilbert space, and prove that the finite-dimensional problem intrinsically converges to the infinite-dimensional counterparts.
- By introducing function-valued reproducing kernel Hilbert space (RKHS) and operator-valued kernel, we further ameliorate iSVGD with precondition information (e.g., Hessian information operator), which is able to accelerate the iSVGD algorithm significantly. This is the first work on such iSVGD algorithm with precondition information to the best of our knowledge.
- We design explicit numerical strategies using the finite-element approach as in [4]. Through theoretical analysis and numerical examples, we demonstrate that the regularity parameter s in our theory should belong to $(0, 0.5)$ and close to 0.5. Taking $s = 0$ leads to algorithms similar to the finite-dimensional case, which conducts unreliable estimates of variances. The scalability of the algorithm follows when the forward and adjoint PDE

solvers are scalable. Hence, the overall algorithm can be efficiently applied to large-scale inverse problems of PDEs.

We present our discussions in the following order. Section 2 makes a short introduction to SVGD in finite-dimensional space. The core of the paper is in Section 3, in which we firstly review the fundamental knowledge of the Hilbert scale and operator-valued kernel. Then, we introduce the Stein operator defined on the separable Hilbert space and prove that the infinite-dimensional version is indeed equivalent to the finite-dimensional version in some limit sense. Based on the Stein operator and the theory of reproducing kernel Hilbert space (RKHS), we derive the update direction of iSVGd. In the last part of this section, we study the change of variables and construct iSVGd with preconditioning operators, which is capable of evidently accelerating the convergence speed of the iSVGd algorithm. In Section 4, we apply our algorithm to an inverse problem governed by a Helmholtz equation. Through comparing the obtained estimates with the results obtained by the pCN and the randomized maximum a posteriori (rMAP) approaches [16, 49], we show the efficiency of the proposed strategies. Finally, we conclude the paper in Section 5.

2. A SHORT REVIEW OF SVGD

Let \mathcal{H} be a separable Hilbert space endowed with its Borel signal algebra $\mathcal{B}(\mathcal{H})$. Let \mathcal{G} represent the solution operator of some PDEs composed with some measurement operator, u the model parameters, and \mathbf{d} the observations. Then, a widely accepted model for the relationship between an observation and its underlying model parameters is the following additive noise model,

$$(2.1) \quad \mathbf{d} = \mathcal{G}(u) + \epsilon,$$

with ϵ representing the noise vector. In the inverse problems, the task is to reconstruct u from the given noisy observation \mathbf{d} .

For statistical inverse problems, we usually need to find a probability measure $\mu^{\mathbf{d}}$ on \mathcal{H} , which is called the posterior probability measure, specified by its density with respect to a prior probability measure μ_0 . Let the Bayesian formula on the Hilbert space be defined by

$$(2.2) \quad \frac{d\mu^{\mathbf{d}}}{d\mu_0}(u) = \frac{1}{Z_{\mathbf{d}}} \exp\left(-\Phi(u; \mathbf{d})\right),$$

where $\Phi(\cdot; \mathbf{d}) : \mathcal{H} \rightarrow \mathbb{R}$ is a continuous function and $\exp(-\Phi(u; \mathbf{d}))$ is integrable with respect to μ_0 . The constant $Z_{\mathbf{d}}$ is chosen to ensure that $\mu^{\mathbf{d}}$ is indeed a probability measure. In the following, the prior measure $\mu_0 := \mathcal{N}(0, \mathcal{C}_0)$ is assumed to be a Gaussian measure defined on \mathcal{H} with \mathcal{C}_0 to be a nonnegative, symmetric and trace class operator. To describe the covariance operator \mathcal{C}_0 clearly, the following Assumption 2.1 [16] is necessary to be first introduced:

Assumption 2.1. *The operator A , densely defined on the separable Hilbert space $\mathcal{H} = L^2(\Omega)$ with $\Omega \subset \mathbb{R}^n$, satisfies the following properties:*

- (1) *A is positive definite, self-adjoint and invertible;*
- (2) *the eigenfunctions $\{\phi_j\}_{j \in \mathbb{N}}$ of A form an orthonormal basis for \mathcal{H} ;*
- (3) *the eigenvalues of A satisfy $\alpha_j \asymp j^{2/n}$;*
- (4) *there is $C > 0$ such that $\sup_{j \in \mathbb{N}} \left(\|\phi_j\|_{L^\infty} + \frac{1}{j^{1/n}} \text{Lip}(\phi_j) \right) \leq C$.*

Assume that $\mathcal{C}_0 = A^{-s}$ with A satisfying Assumption 2.1 and $s > \frac{n}{2}$ and let $(\lambda_k, \varepsilon_k)_{k=1}^{\infty}$ be eigensystem of \mathcal{C}_0 with $\mathcal{C}_0 \varepsilon_k = \lambda_k^2 \varepsilon_k$. Then it can be deduced that $\lambda_k \asymp k^{-s/n}$. Let P^N denote orthogonal projection in \mathcal{H} onto $X^N := \text{span}\{\varepsilon_1, \varepsilon_2, \dots, \varepsilon_N\}$ and Q^N orthogonal projection in \mathcal{H} onto $X^\perp := \text{span}\{\varepsilon_{N+1}, \varepsilon_{N+2}, \dots\}$. Thus $Q^N = \text{Id} - P^N$. Let $u^N := P^N u \in X^N$ and $u^\perp := Q^N u \in X^\perp$. Define $\mathcal{C}_0^N = P^N \mathcal{C}_0 P^N$ and let $\mu_0^N = \mathcal{N}(0, \mathcal{C}_0^N)$ be a finite-dimensional Gaussian measure defined on X^N . With these notations, it can then be introduced that an approximate measure μ^{dN} on X^N defined by

$$(2.3) \quad \frac{d\mu^{dN}}{d\mu_0^N}(u^N) = \frac{1}{Z_{\mathbf{d}}^N} \exp\left(-\Phi(u^N; \mathbf{d})\right),$$

where

$$Z_{\mathbf{d}}^N = \int_{X^N} \exp\left(-\Phi(u^N; \mathbf{d})\right) \mu_0^N(du^N).$$

For more properties of this approximate measure, please refer to Subsection 5.6 in [16]. Because the probability measure μ^{dN} is defined on the finite-dimensional space X^N , it possesses a probability density function p^{dN} defined as follows:

$$(2.4) \quad p^{dN}(u^N) \propto \exp\left(-\Phi(u^N; \mathbf{d}) - \frac{1}{2}\|u^N\|_{\mathcal{C}_0^N}^2\right),$$

where $\|\cdot\|_{\mathcal{C}_0^N}$ represents $\|(\mathcal{C}_0^N)^{-1/2} \cdot\|_{\ell^2}$ with $\|\cdot\|_{\ell^2}$ standing for the usual ℓ^2 -norm.

Variational inference (VI) approximates the target measure p^{dN} using a simpler measure q^N found in a predefined set of measures \mathcal{Q} by minimizing the Kullback-Leibler (KL) divergence, that is,

$$q^{N*} = \underset{q^N \in \mathcal{Q}}{\text{argmin}} \left\{ \text{KL}(q^N \| p^{dN}) = \mathbb{E}_{u^N \sim q^N} [\log q^N(u^N)] - \mathbb{E}_{u^N \sim q^N} [\log p^{dN}(u^N)] \right\}.$$

The choice of the set \mathcal{Q} is critical, and variations of its choice correspond to different types of VI methods. In SVGD, \mathcal{Q} is chosen as follows:

$$\mathcal{Q} = \left\{ q^N(v^N) : \begin{array}{l} q^N \text{ is implicitly defined by } T : X^N \rightarrow X^N \\ \text{with } v^N = T(u^N) \text{ and } u^N \sim q_0^N \end{array} \right\},$$

where T is a smooth one-to-one transform, and u^N is drawn from a tractable reference probability measure $q_0^N(du^N)$. The key idea for constructing SVGD is to introduce the map $T(u^N) := u^N + \epsilon \phi(u^N)$, where ϕ is a smooth function that characterizes the update direction and the scalar ϵ represents the perturbation magnitude. Then, a series of such transforms can be constructed as

$$\begin{aligned} u_1^N = T_0(u_0^N) = u_0^N + \epsilon \phi_0(u_0^N) &\longrightarrow u_2^N = T_1(u_1^N) = u_1^N + \epsilon \phi_1(u_1^N) \longrightarrow \\ &\dots \longrightarrow u_{\ell+1}^N = T_\ell(u_\ell^N) = u_\ell^N + \epsilon \phi_\ell(u_\ell^N) \longrightarrow \dots \end{aligned}$$

These transforms lead to a series of probability measures

$$q_0^N(du^N) \longrightarrow q_1^N(du^N) \longrightarrow \dots \longrightarrow q_\ell^N(du^N) \longrightarrow \dots$$

According to our purpose, we need to ensure that $q_\infty^N(du^N) = p^{dN}(du^N)$. We thus choose the following intuitive smooth transforms:

$$(2.5) \quad \phi_\ell^{N*} = \underset{\phi \in \mathcal{H}_K^N, \|\phi\|_{\mathcal{H}_K^N} \leq 1}{\text{argmax}} \left\{ -\frac{d}{d\epsilon_\ell} \text{KL}(q_{\ell-1}^N \circ T_\ell^{-1} \| p^{dN})|_{\epsilon_\ell=0} \right\},$$

where \mathcal{H}_K^N is the reproducing kernel Hilbert space (RKHS) defined on n -dimensional space with kernel function K . In Liu and Wang's original paper [32], for each smooth function ϕ_ℓ with $\ell \in \mathbb{N}^+$, they prove the following important identity:

$$(2.6) \quad \frac{d}{d\epsilon_\ell} \text{KL}(q_{\ell-1}^N \circ T_\ell^{-1} \| p^{\mathbf{d}N})|_{\epsilon_\ell=0} = -\mathbb{E}_{u^N \sim q_\ell^N} [\mathcal{S}\phi_\ell(u^N)],$$

where

$$(2.7) \quad \mathcal{S}^T \phi_\ell(u^N) = \nabla_{u^N} \log p^{\mathbf{d}N}(u^N)^T \phi_\ell(u^N) + \nabla_{u^N}^T \phi_\ell(u^N).$$

With the above key identity (2.6), Liu and Wang [32] find that the solution of (2.5) is

$$(2.8) \quad \phi_\ell^{N*}(\cdot) \propto \mathbb{E}_{u^N \sim q_\ell^N} [\mathcal{S}K(u^N, \cdot)],$$

where $\mathbb{E}_{u^N \sim q_\ell^N}$ stands for taking expectation with respect to u^N . Similar notations will be employed in the following. Then, the basic SVGD algorithm can be easily constructed, which is listed in Algorithm 1 for reader's convenience. Inspired by

Algorithm 1 Finite-dimensional Stein variational gradient descent

Input: A target probability measure with density function $p^{\mathbf{d}N}(u^N)$ and a set of particles $\{u_i^{N,0}\}_{i=1}^m$.

Output: A set of particles $\{u_i^N\}_{i=1}^m$ that approximates the target probability measure.

for iteration ℓ do

$$u_i^{N,\ell+1} \leftarrow u_i^{N,\ell} + \epsilon_\ell \phi^*(u_i^{N,\ell}),$$

with

$$\phi^*(u^N) = \frac{1}{m} \sum_{j=1}^m \left[K(u_j^{N,\ell}, u^N) \nabla_{u_j^{N,\ell}} \log p^{\mathbf{d}N}(u_j^{N,\ell}) + \nabla_{u_j^{N,\ell}} K(u_j^{N,\ell}, u^N) \right],$$

where ϵ_ℓ is the step size at the ℓ -th iteration.

end for

essential machine learning applications, SVGD type algorithms are widely studied during the past several years [17, 35].

3. CONSTRUCT SVGD ON SEPARABLE HILBERT SPACE

In this section, we first make a short review of some necessary basic knowledge. Then, we introduce some of the corresponding definitions and construct the iSVGd update directions explicitly, which provide the general framework of our iSVGd algorithm. At last, we prove the change of variables theorem and construct iSVGd with preconditioning operators.

3.1. Hilbert scale and function-valued RKHS. Firstly, let us present a brief introduction about the Hilbert scales [18], which are powerful tools for measuring the smoothness of the function parameters. Let $\mathcal{C}_0 : \mathcal{H} \rightarrow \mathcal{H}$ be a self-adjoint, positive-definite, trace class, linear operator with eigensystem $(\lambda_i^2, \varepsilon_i)_{i=1}^\infty$. Then, $\mathcal{D}(\mathcal{C}_0)$ and $\mathcal{R}(\mathcal{C}_0)$ refer to its domain and range, respectively. Considering $\mathcal{H} = \overline{\mathcal{R}(\mathcal{C}_0)} \oplus \mathcal{R}(\mathcal{C}_0)^\perp = \overline{\mathcal{R}(\mathcal{C}_0)}$ (the closure of $\mathcal{R}(\mathcal{C}_0)$), we know that \mathcal{C}_0^{-1} is a densely defined, unbounded, symmetric and positive-definite operator in \mathcal{H} . Let $\langle \cdot, \cdot \rangle_{\mathcal{H}}$ and

$\|\cdot\|_{\mathcal{H}}$ be the inner product and norm defined on the Hilbert space \mathcal{H} , respectively. We define the Hilbert scales $(\mathcal{H}^t)_{t \in \mathbb{R}}$, with $\mathcal{H}^t := \overline{\mathcal{S}_f}^{\|\cdot\|_{\mathcal{H}^t}}$, where

$$\mathcal{S}_f := \bigcap_{n=0}^{\infty} \mathcal{D}(\mathcal{C}_0^{-n}), \quad \langle u, v \rangle_{\mathcal{H}^t} := \langle \mathcal{C}_0^{-t/2} u, \mathcal{C}_0^{-t/2} v \rangle, \quad \|u\|_{\mathcal{H}^t} := \left\| \mathcal{C}_0^{-t/2} u \right\|_{\mathcal{H}}.$$

The norms defined above possess the following properties.

Lemma 3.1. (Proposition 8.19 in [18]) *Let $(\mathcal{H}^t)_{t \in \mathbb{R}}$ be the Hilbert scale induced by the operator \mathcal{C}_0 defined above. Then the following assertions hold:*

- (1) *Let $-\infty < s < t < \infty$. Then the space \mathcal{H}^t is densely and continuously embedded in \mathcal{H}^s .*
- (2) *If $t \geq 0$, then $\mathcal{H}^t = \mathcal{D}(\mathcal{C}_0^{-t/2})$, and \mathcal{H}^{-t} is the dual space of \mathcal{H}^t .*
- (3) *Let $-\infty < q < r < s < \infty$ then the interpolation inequality $\|u\|_{\mathcal{H}^r} \leq \|u\|_{\mathcal{H}^q}^{\frac{s-r}{s-q}} \|u\|_{\mathcal{H}^s}^{\frac{r-q}{s-q}}$ holds when $u \in \mathcal{H}^s$.*

Before giving an introduction of the RKHS, let us specify the meaning of the Hilbert space adjoint operator as follows.

Definition 3.2. [42] Let \mathcal{X} and \mathcal{Y} be Banach space, and T be a bounded linear operator from \mathcal{X} to \mathcal{Y} . The **Banach space adjoint** of T , denoted by T' , is the bounded linear operator from \mathcal{Y}^* to \mathcal{X}^* defined by $(T'\ell)(u) = \ell(Tu)$ for all $\ell \in \mathcal{Y}^*$, $u \in \mathcal{X}$. Let $C_1 : \mathcal{X} \rightarrow \mathcal{X}^*$ the bounded linear functional $\langle u, \cdot \rangle_{\mathcal{X}}$ in \mathcal{X}^* , being the map which assigns to each $u \in \mathcal{X}$, \cdot . Let $C_2 : \mathcal{Y} \rightarrow \mathcal{Y}^*$ be defined similar to C_1 . The operators C_1 and C_2 are conjugate linear isometry which is surjective by the Riesz lemma. Then define the **Hilbert space adjoint** of T be a map $T^* : \mathcal{Y} \rightarrow \mathcal{X}$ by $T^* = C_1^{-1} T' C_2$.

Now, we introduce function-valued positive definite kernels, which constitutes the generally used framework for specifying function-valued RKHS. Following Kadri et al. [29], we focus on separable Hilbert spaces with reproducing operator-valued kernels whose elements are continuous functions, and thus can avoid topological and measurability problems. We denote by \mathcal{X} and \mathcal{Y} the separable Hilbert spaces and by $\mathcal{L}(\mathcal{X}, \mathcal{Y})$ the set of bounded linear operators from \mathcal{X} to \mathcal{Y} . When $\mathcal{X} = \mathcal{Y}$, we write $\mathcal{L}(\mathcal{Y}, \mathcal{Y})$ briefly as $\mathcal{L}(\mathcal{Y})$.

Definition 3.3. (Operator-valued kernel) An $\mathcal{L}(\mathcal{Y})$ -valued kernel \mathbf{K} on $\mathcal{X} \times \mathcal{X}$ is a function $\mathbf{K}(\cdot, \cdot) : \mathcal{X} \times \mathcal{X} \rightarrow \mathcal{L}(\mathcal{Y})$;

- (1) \mathbf{K} is Hermitian if $\forall u, v \in \mathcal{X}$, $\mathbf{K}(u, v) = \mathbf{K}(v, u)^*$,
- (2) \mathbf{K} is nonnegative on \mathcal{X} if it is Hermitian and for every natural number r and all $\{(u_i, v_i)_{i=1, \dots, r}\} \in \mathcal{X} \times \mathcal{Y}$, the matrix with ij -th entry $\langle \mathbf{K}(u_i, u_j) v_i, v_j \rangle_{\mathcal{Y}}$ is nonnegative (positive-definite).

Now we are ready to present the definition of function-valued RKHS.

Definition 3.4. (Function-valued RKHS) Let \mathcal{X} and \mathcal{Y} be two separable Hilbert spaces. A Hilbert space \mathcal{F} of functions from \mathcal{X} to \mathcal{Y} is called a reproducing kernel Hilbert space if there is a nonnegative $\mathcal{L}(\mathcal{Y})$ -valued kernel \mathbf{K} on $\mathcal{X} \times \mathcal{X}$ such that:

- (1) the function $v \mapsto \mathbf{K}(u, v)g$ belongs to \mathcal{F} for all $v, u \in \mathcal{X}$ and $g \in \mathcal{Y}$;
- (2) for every $f \in \mathcal{F}$, $u \in \mathcal{X}$ and $g \in \mathcal{Y}$, we have $\langle f(w), g \rangle_{\mathcal{Y}} = \langle f(\cdot), \mathbf{K}(w, \cdot)g \rangle_{\mathcal{F}}$.

On account of (2) in the above definition, the kernel is called the reproducing kernel of \mathcal{F} . Throughout this paper, we assume that the kernel \mathbf{K} is *locally bounded and separately continuous*, which guarantees that \mathcal{F} is a subspace of $C(\mathcal{X}, \mathcal{Y})$ (the vector space of continuous functions from \mathcal{X} to \mathcal{Y}). Such a kernel is qualified as Mercer [7, 8]. For Mercer kernel, we list the following fundamental results.

Theorem 3.5. [29] (*Bijection between function-valued RKHS and operator-valued kernel*) A $\mathcal{L}(\mathcal{Y})$ -valued Mercer kernel \mathbf{K} on \mathcal{X}^2 is the reproducing kernel of some Hilbert space \mathcal{F} , if and only if it is nonnegative.

In order to provide some intuitions about RKHS, we list the outline of the proof as follows: We assume that \mathcal{F}_0 represents the space of all \mathcal{Y} -valued functions F of the form $F(\cdot) = \sum_{i=1}^m \mathbf{K}(u_i, \cdot)v_i$, where $u_i \in \mathcal{X}$ and $v_i \in \mathcal{Y}$, with the following inner product $\langle F(\cdot), G(\cdot) \rangle_{\mathcal{F}_0} = \sum_{i=1}^m \sum_{j=1}^n \langle \mathbf{K}(u_i, \tilde{u}_j)v_i, \tilde{v}_j \rangle_{\mathcal{Y}}$ defined for any $G(\cdot) = \sum_{j=1}^n \mathbf{K}(\tilde{u}_j, \cdot)\tilde{v}_j$ with $\tilde{u}_j \in \mathcal{X}$ and $\tilde{v}_j \in \mathcal{Y}$. Then we can show that $(\mathcal{F}_0, \langle \cdot, \cdot \rangle_{\mathcal{F}_0})$ is a pre-Hilbert space. Finally, we complete this pre-Hilbert space to construct the Hilbert space \mathcal{F} of \mathcal{Y} -valued functions which is just the required RKHS. A complete proof of Theorem 3.5 can be found in [29]. At last, We refer the readers to [3, 7, 8, 29, 38] for more details about the function-valued RKHS.

3.2. Construct iSVGd. After brief introductions about the Hilbert scale and operator-valued kernels, we are ready to derive an infinite-dimensional version of SVGD (iSVGd). For a function variable u , let D_u denote the Fréchet derivative and D_{u_k} denote the directional derivative in the k th direction. If there is no ambiguity, the notations D and D_k will be used instead of D_u and D_{u_k} for conciseness. In the following, we briefly write $\Phi(u; \mathbf{d})$ as $\Phi(u)$ and set

$$(3.1) \quad V(u) = \Phi(u) + \frac{1}{2} \|u\|_{\mathcal{H}^1}^2.$$

Before going further, let us provide some assumptions on the potential functional Φ which is crucial for our theory.

Assumption 3.6. *There exist constants $M_i \in \mathbb{R}^+$, $i \leq 4$ such that for all $u \in \mathcal{X} \subset \mathcal{H}$, the functional $\Phi : \mathcal{X} \rightarrow \mathbb{R}$ satisfies*

$$\begin{aligned} -M_1 &\leq \Phi(u) \leq M_2(1 + \|u\|_{\mathcal{X}}^2); \\ \|D\Phi(u)\|_{\mathcal{X}^*} &\leq M_3(1 + \|u\|_{\mathcal{X}}), \quad \|D\Phi(u)\|_{\mathcal{H}} \leq M_3(1 + \|u\|_{\mathcal{H}}); \\ \|D^2\Phi(u)\|_{\mathcal{L}(\mathcal{X}, \mathcal{X}^*)} &\leq M_4, \quad \|D^2\Phi(u)\|_{\mathcal{L}(\mathcal{H}, \mathcal{H})} \leq M_4. \end{aligned}$$

The above assumption is similar to Assumption 4 given in [16], which can be verified for many problems [16]. We now optimize ϕ in the unit ball of a general function-valued RKHS $\mathcal{H}_{\mathbf{K}}$ with an operator valued kernel $\mathbf{K}(u, u') \in \mathcal{L}(\mathcal{Y})$:

$$(3.2) \quad \phi_{\mathbf{K}}^* = \operatorname{argmax}_{\phi \in \mathcal{H}_{\mathbf{K}}} \{\mathbb{E}_{u \sim \mu}[\mathcal{S}\phi(u)], \text{ s.t. } \|\phi\|_{\mathcal{H}_{\mathbf{K}}} \leq 1 \text{ and } D\phi : \mathcal{X} \rightarrow \mathcal{L}_1(\mathcal{X}, \mathcal{Y})\},$$

where \mathcal{S} is the generalized Stein operator defined as follows:

$$(3.3) \quad \mathcal{S}\phi(u) = \langle DV(u), \phi(u) \rangle_{\mathcal{Y}} + \sum_{k=1}^{\infty} D_k \langle \phi(u), e_k \rangle_{\mathcal{Y}},$$

and $\mathcal{L}_1(\mathcal{X}, \mathcal{Y})$ denotes the set of all trace class operators from \mathcal{X} to \mathcal{Y} . Here, $\{e_k\}_{k=1}^{\infty}$ stands for an orthonormal basis of space \mathcal{Y} and μ is a probability measure defined on \mathcal{H} . To ensure the appropriateness of (3.2), we assume that $\phi : \mathcal{X} \rightarrow \mathcal{Y}$ is Fréchet differentiable, and the derivative is continuous.

Remark 3.7. In the classical finite-dimensional case, the operator $D\phi(u)$ naturally belongs to $\mathcal{L}_1(\mathcal{X}, \mathcal{Y})$ (see Appendix C in [15]).

We need the following assumption for the function-valued kernels, which includes numerous useful kernels, e.g., radial basis function (RBF) kernel.

Assumption 3.8. *Let \mathcal{X} , \mathcal{Y} , and \mathcal{H} be three separable Hilbert spaces. For $s \in [0, 1]$, we assume that $\mathcal{H}^{-s-1} \subset \mathcal{Y}$ and*

$$(3.4) \quad \sup_{u \in \mathcal{X}} \|\mathbf{K}(u, u)\|_{\mathcal{L}(\mathcal{Y})} < \infty.$$

To illustrate the reasonability of (3.2) and (3.3), we prove the following Theorem 3.9. For each particle u , we assume that $u \in \mathcal{H}^{1-s}$, which is based on the following two considerations:

- SVGD with only one particle is just an optimization algorithm for finding maximum a posteriori (MAP) estimate. The MAP estimate belongs to the separable Hilbert space \mathcal{H}^1 .
- For the prior probability measure, the space \mathcal{H}^1 has zero measure [15]. Intuitively, if all particles belong to \mathcal{H}^1 , the particles tend to concentrate around a small set that lead to unreliable estimates of the variance. Hence, we prefer to assume that the particles belong to a larger space contains \mathcal{H}^1 .

Theorem 3.9. *The generalized Stein operator (3.3) defined on \mathcal{Y} can be obtained by taking $N \rightarrow \infty$ in the following finite-dimensional Stein operator*

$$(3.5) \quad \mathcal{S}^N \phi^N(u^N) = \langle DV(u^N), \phi^N(u^N) \rangle_{\mathcal{Y}} + \sum_{k=1}^N D_k \langle \phi^N(u^N), e_k \rangle_{\mathcal{Y}},$$

where $\phi^N := P^N \circ \phi$.

Proof. By straightforward calculations, we have

$$(3.6) \quad \begin{aligned} \mathcal{S}\phi(u) - \mathcal{S}^N \phi^N(u^N) &= \left(\langle DV(u), \phi(u) \rangle_{\mathcal{Y}} - \langle DV(u^N), \phi^N(u^N) \rangle_{\mathcal{Y}} \right) \\ &+ \left(\sum_{k=1}^{\infty} D_k \langle \phi(u), e_k \rangle_{\mathcal{Y}} - \sum_{k=1}^N D_k \langle \phi^N(u^N), e_k \rangle_{\mathcal{Y}} \right) \\ &= \text{I} + \text{II}. \end{aligned}$$

For term I, we have

$$(3.7) \quad \begin{aligned} \text{I} &= \langle D(V(u) - V(u^N)), \phi^N(u^N) \rangle_{\mathcal{Y}} + \langle DV(u), \phi(u) - \phi^N(u^N) \rangle_{\mathcal{Y}} \\ &= \text{I}_1(N) + \text{I}_2(N). \end{aligned}$$

For term $\text{I}_1(N)$, we find that

$$(3.8) \quad \text{I}_1(N) = \langle D(\Phi(u) - \Phi(u^N)), \phi^N(u^N) \rangle_{\mathcal{Y}} + \langle \mathcal{C}_0^{-1/2}(u - u^N), \mathcal{C}_0^{-1/2} \phi^N(u^N) \rangle_{\mathcal{Y}},$$

where the second term on the right-hand side could be understood as white noise mapping [41]. According to Assumption 3.6, we know that

$$(3.9) \quad \begin{aligned} \lim_{N \rightarrow \infty} \|D(\Phi(u) - \Phi(u^N))\|_{\mathcal{Y}} &\leq \lim_{N \rightarrow \infty} C \|\mathcal{C}_0^{\frac{1+s}{2}} D(\Phi(u) - \Phi(u^N))\|_{\mathcal{H}} \\ &\leq \lim_{N \rightarrow \infty} C \|D(\Phi(u) - \Phi(u^N))\|_{\mathcal{H}} = 0, \end{aligned}$$

where C is a generic constant that can be different from line to line. Hence, we obtain

$$(3.10) \quad \lim_{N \rightarrow \infty} \langle D(\Phi(u) - \Phi(u^N)), \phi^N(u^N) \rangle_{\mathcal{Y}} = 0.$$

Take $u_m \in \mathcal{H}^2$ such that $u_m \rightarrow u$ in \mathcal{H}^{1-s} . Then we have

$$\begin{aligned} \langle \mathcal{C}_0^{-1/2}(u - u^N), \mathcal{C}_0^{-1/2} \phi^N(u^N) \rangle_{\mathcal{Y}} &= \lim_{m \rightarrow \infty} \langle \mathcal{C}_0^{-1/2}(u_m - u_m^N), \mathcal{C}_0^{-1/2} \phi^N(u^N) \rangle_{\mathcal{Y}} \\ &= \lim_{m \rightarrow \infty} \langle P^N \mathcal{C}_0^{-1}(u_m - u_m^N), \phi(u^N) \rangle_{\mathcal{Y}} \\ &= \lim_{m \rightarrow \infty} \langle \phi(\cdot), \mathbf{K}(u^N, \cdot) P^N \mathcal{C}_0^{-1}(u_m - u_m^N) \rangle_{\mathcal{H}_{\mathbf{K}}}. \end{aligned}$$

We can have the following estimates:

$$\begin{aligned} &\langle \phi(\cdot), \mathbf{K}(u^N, \cdot) P^N \mathcal{C}_0^{-1}(u_m - u_m^N) \rangle_{\mathcal{H}_{\mathbf{K}}} \leq \\ &\quad \langle \phi(\cdot), \phi(\cdot) \rangle_{\mathcal{H}_{\mathbf{K}}} \langle \mathbf{K}(u^N, \cdot) P^N \mathcal{C}_0^{-1}(u_m - u_m^N), \mathbf{K}(u^N, \cdot) P^N \mathcal{C}_0^{-1}(u_m - u_m^N) \rangle_{\mathcal{H}_{\mathbf{K}}} \\ &\leq \langle \phi(\cdot), \phi(\cdot) \rangle_{\mathcal{H}_{\mathbf{K}}} \langle P^N \mathbf{K}(u^N, u^N) P^N \mathcal{C}_0^{-1}(u_m - u_m^N), \mathcal{C}_0^{-1}(u_m - u_m^N) \rangle_{\mathcal{Y}} \\ &\leq C \langle \phi(\cdot), \phi(\cdot) \rangle_{\mathcal{H}_{\mathbf{K}}} \|\mathcal{C}_0^{-1}(u_m - u_m^N)\|_{\mathcal{Y}}^2 \\ &\leq C \langle \phi(\cdot), \phi(\cdot) \rangle_{\mathcal{H}_{\mathbf{K}}} \|\mathcal{C}_0^{-\frac{1-s}{2}}(u_m - u_m^N)\|_{\mathcal{H}}^2. \end{aligned}$$

With $u_m - u_m^N$ replaced by $(u_m - u_m^N) - (u - u^N)$, we can deduce that

$$(3.11) \quad \begin{aligned} \langle \mathcal{C}_0^{-1/2}(u - u^N), \mathcal{C}_0^{-1/2} \phi^N(u^N) \rangle_{\mathcal{Y}} &= \lim_{m \rightarrow \infty} \langle \phi(\cdot), \mathbf{K}(u^N, \cdot) P^N \mathcal{C}_0^{-1}(u_m - u_m^N) \rangle_{\mathcal{H}_{\mathbf{K}}} \\ &= \langle \phi(\cdot), \mathbf{K}(u^N, \cdot) P^N \mathcal{C}_0^{-1}(u - u^N) \rangle_{\mathcal{H}_{\mathbf{K}}}. \end{aligned}$$

Hence, we obtain

$$(3.12) \quad \begin{aligned} &\lim_{N \rightarrow \infty} \langle \mathcal{C}_0^{-1/2}(u - u^N), \mathcal{C}_0^{-1/2} \phi^N(u^N) \rangle_{\mathcal{Y}} \\ &= \lim_{N \rightarrow \infty} \langle \phi(\cdot), \mathbf{K}(u^N, \cdot) P^N \mathcal{C}_0^{-1}(u - u^N) \rangle_{\mathcal{H}_{\mathbf{K}}} \\ &\leq \lim_{N \rightarrow \infty} \langle \phi(\cdot), \phi(\cdot) \rangle_{\mathcal{H}_{\mathbf{K}}} \langle P^N \mathbf{K}(u^N, u^N) P^N \mathcal{C}_0^{-1}(u - u^N), \mathcal{C}_0^{-1}(u - u^N) \rangle_{\mathcal{Y}} \\ &\leq C \langle \phi(\cdot), \phi(\cdot) \rangle_{\mathcal{H}_{\mathbf{K}}} \lim_{N \rightarrow \infty} \|\mathcal{C}_0^{-\frac{1-s}{2}}(u - u^N)\|_{\mathcal{H}}^2 = 0. \end{aligned}$$

Plugging (3.10) and (3.12) into (3.8), we arrive at $\lim_{N \rightarrow \infty} I_1(N) = 0$. For term $I_2(N)$, it can be decomposed as follows:

$$(3.13) \quad I_2(N) = \langle D\Phi(u), \phi(x) - \phi^N(u^N) \rangle_{\mathcal{Y}} + \langle \mathcal{C}_0^{-1/2}u, \mathcal{C}_0^{-1/2}(\phi(u) - \phi^N(u^N)) \rangle_{\mathcal{Y}}.$$

Based on the continuity of ϕ , we have $\lim_{N \rightarrow \infty} \langle D\Phi(u), \phi(x) - \phi^N(u^N) \rangle_{\mathcal{Y}} = 0$. Using similar estimates as for deriving (3.11), we obtain

$$(3.14) \quad \begin{aligned} &\langle \mathcal{C}_0^{-1/2}u, \mathcal{C}_0^{-1/2}(\phi(u) - \phi^N(u^N)) \rangle_{\mathcal{Y}} \\ &= \langle \phi(\cdot), \mathbf{K}(u, \cdot) \mathcal{C}_0^{-1}u \rangle_{\mathcal{H}_{\mathbf{K}}} - \langle \phi(\cdot), \mathbf{K}(u^N, \cdot) P^N \mathcal{C}_0^{-1}u \rangle_{\mathcal{H}_{\mathbf{K}}}. \end{aligned}$$

According to the continuity of $\mathbf{K}(\cdot, \cdot)$, we obtain

$$(3.15) \quad \lim_{N \rightarrow \infty} \langle \mathcal{C}_0^{-1/2}u, \mathcal{C}_0^{-1/2}(\phi(u) - \phi^N(u^N)) \rangle_{\mathcal{Y}} = 0.$$

Now, we conclude that $\lim_{N \rightarrow \infty} I_2(N) = 0$. For term II, we have

$$(3.16) \quad \text{II} = \sum_{k=1}^N D_k \langle \phi(u) - \phi(u^N), e_k \rangle_{\mathcal{Y}} + \sum_{k=N+1}^{\infty} D_k \langle \phi(u), e_k \rangle_{\mathcal{Y}}.$$

Let $\{\varphi_k\}_{k=1}^{\infty}$ be an orthonormal basis in \mathcal{X} , and then we have

$$(3.17) \quad \sum_{k=N+1}^{\infty} D_k \langle \phi(u), e_k \rangle_{\mathcal{Y}} = \sum_{k=N+1}^{\infty} \langle D\phi(u)\varphi_k, e_k \rangle_{\mathcal{Y}} \rightarrow 0 \quad \text{as } N \rightarrow \infty,$$

where we used the condition $D\phi(u) \in \mathcal{L}_1(\mathcal{X}, \mathcal{Y})$. For the first term on the right-hand side of (3.16), we find that

$$(3.18) \quad \sum_{k=1}^N D_k \langle \phi(u) - \phi(u^N), e_k \rangle_{\mathcal{Y}} = \sum_{k=1}^N \langle (D\phi(u) - D\phi(u^N))\varphi_k, e_k \rangle_{\mathcal{Y}}.$$

Due to the continuity of the Fréchet derivative of ϕ , we know that the above summation goes to 0 as $N \rightarrow \infty$. Combining estimates about I and II, we complete the proof. \square

The following theorem gives the iSVGd update directions explicitly that is essential for constructing iSVGd.

Theorem 3.10. *Let $\mathbf{K}(\cdot, \cdot) : \mathcal{X}^2 \rightarrow \mathcal{L}(\mathcal{Y})$ be a positive definite kernel that is Fréchet differentiable on both variables. In addition, we assume that*

$$(3.19) \quad \mathbb{E}_{u \sim \mu} \left[D_{u'} \mathbf{K}(u, u') \mathcal{C}_0^{-1/2} g + \sum_{k=1}^{\infty} D_k D_{u'} \mathbf{K}(u, u') e_k \right]$$

belongs to $\mathcal{L}_1(\mathcal{X}, \mathcal{Y})$ for each $u' \in \mathcal{X}$ and $g \in \mathcal{H}^{-s}$. Then, the optimal $\phi_{\mathbf{K}}^*$ in (3.2) is

$$(3.20) \quad \phi_{\mathbf{K}}^*(\cdot) \propto \mathbb{E}_{u \sim \mu} \left[\mathbf{K}(u, \cdot) (D\Phi(u) + \mathcal{C}_0^{-1}u) + \sum_{k=1}^{\infty} D_k \mathbf{K}(u, \cdot) e_k \right],$$

where $\{e_k\}_{k=1}^{\infty}$ is an orthonormal basis of \mathcal{Y} and the term $\mathbf{K}(u, \cdot) \mathcal{C}_0^{-1}u$ should be understood in the limiting sense as follows:

$$(3.21) \quad \mathbf{K}(u, \cdot) \mathcal{C}_0^{-1}u := \lim_{m \rightarrow \infty} \mathbf{K}(u, \cdot) \mathcal{C}_0^{-1}u_m,$$

where the limit is taken in $\mathcal{H}_{\mathbf{K}}$ and $\{u_m\}_{m=1}^{\infty} \subset \mathcal{H}^2$ such that $\|\mathcal{C}_0^{-\frac{1-s}{2}}(u_m - u)\|_{\mathcal{H}} \rightarrow 0$ as $m \rightarrow \infty$.

Proof. Firstly, by taking $\phi(u)$ as an element in $\mathcal{H}_{\mathbf{K}}$, we have

$$(3.22) \quad \langle DV(u), \phi(u) \rangle_{\mathcal{Y}} = \langle D\Phi(u), \phi(u) \rangle_{\mathcal{Y}} + \langle \mathcal{C}_0^{-1/2}u, \mathcal{C}_0^{-1/2}\phi(u) \rangle_{\mathcal{Y}} = \text{I} + \text{II},$$

where term II should be understood as the white noise mapping. For term I, we have

$$(3.23) \quad \text{I} = \langle \phi(\cdot), \mathbf{K}(u, \cdot) D\Phi(u) \rangle_{\mathcal{H}_{\mathbf{K}}},$$

where proposition (2) in Definition 3.4 has been employed. For term II, we take $u_m \in \mathcal{H}^2$ such that $\lim_{m \rightarrow \infty} \|\mathcal{C}_0^{-\frac{1-s}{2}}(u_m - u)\|_{\mathcal{H}} = 0$. Obviously, we have

$$(3.24) \quad \langle \mathcal{C}_0^{-1/2}u_m, \mathcal{C}_0^{-1/2}\phi(u) \rangle_{\mathcal{Y}} = \langle \mathcal{C}_0^{-1}u_m, \phi(u) \rangle_{\mathcal{Y}} = \langle \phi(\cdot), \mathbf{K}(u, \cdot) \mathcal{C}_0^{-1}u_m \rangle_{\mathcal{H}_{\mathbf{K}}}.$$

Because

$$\begin{aligned}
& |\langle \phi(\cdot), \mathbf{K}(u, \cdot) \mathcal{C}_0^{-1} u_m \rangle_{\mathcal{H}_{\mathbf{K}}} - \langle \phi(\cdot), \mathbf{K}(u, \cdot) \mathcal{C}_0^{-1} u \rangle_{\mathcal{H}_{\mathbf{K}}} |^2 \\
& \leq \langle \phi(\cdot), \phi(\cdot) \rangle_{\mathcal{H}_{\mathbf{K}}} \langle \mathbf{K}(u, \cdot) \mathcal{C}_0^{-1} (u_m - u), \mathbf{K}(u, \cdot) \mathcal{C}_0^{-1} (u_m - u) \rangle_{\mathcal{H}_{\mathbf{K}}} \\
& = \langle \phi(\cdot), \phi(\cdot) \rangle_{\mathcal{H}_{\mathbf{K}}} \langle \mathbf{K}(u, u) \mathcal{C}_0^{-1} (u_m - u), \mathcal{C}_0^{-1} (u_m - u) \rangle_{\mathcal{Y}} \\
& \leq \langle \phi(\cdot), \phi(\cdot) \rangle_{\mathcal{H}_{\mathbf{K}}} \langle \mathbf{K}(u, u) \mathcal{C}_0^{-1} (u_m - u), \mathcal{C}_0^{-1} (u_m - u) \rangle_{\mathcal{Y}} \\
& \leq C \langle \phi(\cdot), \phi(\cdot) \rangle_{\mathcal{H}_{\mathbf{K}}} \| \mathcal{C}_0^{-\frac{1-s}{2}} (u_m - u) \|_{\mathcal{H}}^2,
\end{aligned}$$

we find that $\lim_{m \rightarrow \infty} \langle \phi(\cdot), \mathbf{K}(u, \cdot) \mathcal{C}_0^{-1} u_m \rangle_{\mathcal{H}_{\mathbf{K}}} = \langle \phi(\cdot), \mathbf{K}(u, \cdot) \mathcal{C}_0^{-1} u \rangle_{\mathcal{H}_{\mathbf{K}}}$. Hence, let $m \rightarrow \infty$ in (3.24), we have

$$(3.25) \quad \langle \mathcal{C}_0^{-1/2} u, \mathcal{C}_0^{-1/2} \phi(u) \rangle_{\mathcal{Y}} = \langle \phi(\cdot), \mathbf{K}(u, \cdot) \mathcal{C}_0^{-1} u \rangle_{\mathcal{H}_{\mathbf{K}}}.$$

Inserting (3.25) and (3.23) into (3.22), we obtain

$$(3.26) \quad \begin{aligned} \langle DV(u), \phi(u) \rangle_{\mathcal{Y}} &= \langle \phi(\cdot), \mathbf{K}(u, \cdot) D\Phi(u) + \mathbf{K}(u, \cdot) \mathcal{C}_0^{-1} u \rangle_{\mathcal{H}_{\mathbf{K}}} \\ &= \langle \phi(\cdot), \mathbf{K}(u, \cdot) DV(u) \rangle_{\mathcal{H}_{\mathbf{K}}}. \end{aligned}$$

Secondly, let us calculate the second term on the right-hand side of (3.3) as follows:

$$(3.27) \quad \sum_{k=1}^{\infty} D_k \langle \phi(u), e_k \rangle_{\mathcal{Y}} = \sum_{k=1}^{\infty} D_k \langle \phi(\cdot), \mathbf{K}(u, \cdot) e_k \rangle_{\mathcal{H}_{\mathbf{K}}}.$$

Since

$$(3.28) \quad \begin{aligned} D_k \langle \phi(\cdot), \mathbf{K}(u, \cdot) e_k \rangle_{\mathcal{H}_{\mathbf{K}}} &= \lim_{\epsilon \rightarrow 0} \frac{1}{\epsilon} \langle \phi(\cdot), \mathbf{K}(u + \epsilon \varphi_k, \cdot) e_k - \mathbf{K}(u, \cdot) e_k \rangle_{\mathcal{H}_{\mathbf{K}}} \\ &= \langle \phi(\cdot), D_k \mathbf{K}(u, \cdot) e_k \rangle_{\mathcal{H}_{\mathbf{K}}}, \end{aligned}$$

we have

$$(3.29) \quad \sum_{k=1}^{\infty} D_k \langle \phi(u), e_k \rangle_{\mathcal{Y}} = \left\langle \phi(\cdot), \sum_{k=1}^{\infty} D_k \mathbf{K}(u, \cdot) e_k \right\rangle_{\mathcal{H}_{\mathbf{K}}}.$$

Combining (3.26) and (3.29) with (3.3), we obtain

$$(3.30) \quad \mathcal{S}\phi(u) = \left\langle \phi(\cdot), \mathbf{K}(u, \cdot) DV(u) + \sum_{k=1}^{\infty} D_k \mathbf{K}(u, \cdot) e_k \right\rangle_{\mathcal{H}_{\mathbf{K}}}.$$

Thus, the optimization problem (3.2) possesses a solution $\phi_{\mathbf{K}}^*(\cdot)$ satisfying

$$(3.31) \quad \phi_{\mathbf{K}}^*(\cdot) \propto \mathbb{E}_{u \sim \mu} \left[\mathbf{K}(u, \cdot) DV(u) + \sum_{k=1}^{\infty} D_k \mathbf{K}(u, \cdot) e_k \right].$$

Based on condition (6.1), we know that $D\phi_{\mathbf{K}}^*(u)$ belongs to $\mathcal{L}_1(\mathcal{X}, \mathcal{Y})$ for each $u \in \mathcal{X}$, which completes the proof. \square

Remark 3.11. It should be noted that assumption (6.1) given in Theorem 3.10 can be verified for many useful kernels. Specifically, we provide additional illustrations about this issue in the supplementary materials.

With Theorem 3.10 at hand, we construct a series of transforms as follows:

$$(3.32) \quad T_{\ell}(u) = u + \epsilon_{\ell} \mathbb{E}_{u' \sim \mu_{\ell}} \left[\mathbf{K}(u', u) DV(u') + \sum_{k=1}^{\infty} D_{(u')_k} \mathbf{K}(u', u) e_k \right]$$

with $\ell = 1, 2, \dots$. In practice, we draw a set of particles $\{u_i^0\}_{i=1}^m$ from some initial measure, and then iteratively update the particles with an empirical version of the above transform in which the expectation under μ_ℓ is approximated by the empirical mean of particles $\{u_i^\ell\}_{i=1}^m$ at the ℓ -th iteration. We summarize the constructed iSVGd in Algorithm 2.

Algorithm 2 Infinite-dimensional Stein variational gradient descent (iSVGd)

Input: A target probability measure μ^d that is absolutely continuous w.r.t the Gaussian measure $\mu_0 = \mathcal{N}(0, \mathcal{C}_0)$ with $\frac{d\mu^d}{d\mu_0}(u) \propto \exp(-\Phi(u))$ and a set of particles $\{u_i^0\}_{i=1}^m$.

Output: A set of particles $\{u_i\}_{i=1}^m$ that approximates the target probability measure.

for iteration ℓ do

$$u_i^{\ell+1} \leftarrow u_i^\ell + \epsilon_\ell \phi^*(u_i^\ell),$$

with

$$\phi^*(u) = \frac{1}{m} \sum_{j=1}^m \left[\mathbf{K}(u_j^\ell, u) (D\Phi(u_j^\ell) + \mathcal{C}_0^{-1} u_j^\ell) + \sum_{k=1}^{\infty} D_{(u_j^\ell)_k} \mathbf{K}(u_j^\ell, u) e_k \right]$$

end for

3.3. iSVGd with precondition information. Relying on the theorems illustrated in Subsection 3.2, we can construct iSVGd with preconditioning operator along the lines shown in [48] for finite-dimensional SVGd. Firstly let us give a theorem concerned with the change of variables.

Theorem 3.12. *Let \mathcal{X} and \mathcal{Y} be two separable Hilbert spaces. Assume \mathcal{F}_0 be a RKHS with a nonnegative $\mathcal{L}(\mathcal{Y})$ -valued kernel $\mathbf{K}_0 : \mathcal{X} \times \mathcal{X} \rightarrow \mathcal{L}(\mathcal{Y})$. Let $\tilde{\mathcal{X}}$ and $\tilde{\mathcal{Y}}$ be two separable Hilbert spaces, and \mathcal{F} be the set of functions from $\tilde{\mathcal{X}}$ to $\tilde{\mathcal{Y}}$ formed by*

$$(3.33) \quad \phi(u) = \mathbf{M}(u)\phi_0(t(u)) \quad \forall \phi_0 \in \mathcal{F}_0,$$

where $\mathbf{M} : \tilde{\mathcal{X}} \rightarrow \mathcal{L}(\mathcal{Y}, \tilde{\mathcal{Y}})$ is a fixed operator-valued function and we assume that $\mathbf{M}(u)$ is an invertible operator for all $u \in \tilde{\mathcal{X}}$, and $t : \tilde{\mathcal{X}} \rightarrow \mathcal{X}$ is a fixed Fréchet differentiable one-to-one mapping. For all $\phi, \phi' \in \mathcal{F}$, we can identify a unique $\phi_0, \phi'_0 \in \mathcal{F}_0$ such that $\phi(u) = \mathbf{M}(u)\phi_0(t(u))$ and $\phi'(u) = \mathbf{M}(u)\phi'_0(t(u))$. Define the inner product on \mathcal{F} via $\langle \phi, \phi' \rangle_{\mathcal{F}} = \langle \phi_0, \phi'_0 \rangle_{\mathcal{F}_0}$, and then \mathcal{F} is also a function-valued RKHS, whose function-valued kernel is

$$(3.34) \quad \mathbf{K}(u, u') = \mathbf{M}(u') \mathbf{K}_0(t(u), t(u')) \mathbf{M}(u)^*,$$

where $\mathbf{M}(u)^*$ denotes the Hilbert space adjoint.

Proof. Let $\{(u_i, g_i)_{i=1, \dots, N}\} \subset \tilde{\mathcal{X}} \times \tilde{\mathcal{Y}}$, and we have the following equality

$$(3.35) \quad \begin{aligned} \langle \mathbf{K}(u_i, u_j) g_i, g_j \rangle_{\tilde{\mathcal{Y}}} &= \langle \mathbf{M}(u_j) \mathbf{K}_0(t(u_i), t(u_j)) \mathbf{M}(u_i)^* g_i, g_j \rangle_{\tilde{\mathcal{Y}}} \\ &= \langle \mathbf{K}_0(t(u_i), t(u_j)) \mathbf{M}(u_i)^* g_i, \mathbf{M}(u_j)^* g_j \rangle_{\mathcal{Y}}. \end{aligned}$$

Then, the nonnegative $\mathbf{K}(\cdot, \cdot)$ follows from the nonnegative property of $\mathbf{K}_0(\cdot, \cdot)$. In order to prove the theorem, we need to verify the two conditions shown in Definition

3.4. For every $u, v \in \tilde{\mathcal{X}}$ and $g \in \tilde{\mathcal{Y}}$, we consider the function $f(v) = \mathbf{K}(u, v)g = \mathbf{M}(v)\mathbf{K}_0(t(u), t(v))\mathbf{M}(u)^*g$. Because of $\mathbf{M}(u)^*g \in \mathcal{Y}$, we easily obtain

$$\mathbf{K}_0(t(u), t(v))\mathbf{M}(u)^*g \in \mathcal{F}_0.$$

According to (3.33), we conclude that $f(\cdot) \in \mathcal{F}$. Secondly, let us verify the reproducing property of $\mathbf{K}(\cdot, \cdot)$. For every $u \in \tilde{\mathcal{X}}, g \in \tilde{\mathcal{Y}}$, and $\phi \in \mathcal{F}$, we have

$$\begin{aligned} \langle \phi(u), g \rangle_{\tilde{\mathcal{Y}}} &= \langle \mathbf{M}(u)\phi_0(t(u)), g \rangle_{\tilde{\mathcal{Y}}} = \langle \phi_0(t(u)), \mathbf{M}(u)^*g \rangle_{\mathcal{Y}} \\ &= \langle \phi_0(\cdot), \mathbf{K}_0(t(u), \cdot)\mathbf{M}(u)^*g \rangle_{\mathcal{F}_0} \\ &= \langle \mathbf{M}(\cdot)\phi_0(t(\cdot)), \mathbf{M}(\cdot)\mathbf{K}_0(t(u), t(\cdot))\mathbf{M}(u)^*g \rangle_{\mathcal{F}} \\ &= \langle \phi(\cdot), \mathbf{K}(u, \cdot)g \rangle_{\mathcal{F}}, \end{aligned}$$

where the fourth equality follows from

$$\langle \phi, \phi' \rangle_{\mathcal{F}} = \langle \phi_0, \phi'_0 \rangle_{\mathcal{F}_0}$$

with $\phi'_0(\cdot) = \mathbf{K}_0(t(u), \cdot)\mathbf{M}(u)^*g$. \square

We now present a key result, which characterizes the change of kernels when we apply invertible variable transforms on the iSVG D trajectory.

Theorem 3.13. *Let $\mathcal{H}, \tilde{\mathcal{H}}, \mathcal{X}, \tilde{\mathcal{X}}, \mathcal{Y}$, and $\tilde{\mathcal{Y}}$ be separable Hilbert spaces satisfying $\mathcal{X} \subset \mathcal{Y}, \tilde{\mathcal{X}} \subset \tilde{\mathcal{Y}}, \mathcal{X} \subset \tilde{\mathcal{Y}}, \tilde{\mathcal{X}} \subset \mathcal{Y}$. Assume that Assumptions 3.8 hold true for space triple $(\mathcal{X}, \mathcal{Y}, \mathcal{H})$ and $(\tilde{\mathcal{X}}, \tilde{\mathcal{Y}}, \tilde{\mathcal{H}})$ with two fixed parameters $s \in [0, 1/2]$ respectively. Let $T \in \mathcal{L}(\mathcal{Y}, \tilde{\mathcal{Y}})$ and, in addition, assume that T is also a bounded operator when restricted to be an operator from \mathcal{X} to $\tilde{\mathcal{X}}$. Let $\mu, \mu^{\mathbf{d}}$ be two probability measures and $\tilde{\mu}, \tilde{\mu}^{\mathbf{d}}$ be the measures of $\tilde{u} = Tu$ when u is drawn from $\mu, \mu^{\mathbf{d}}$, respectively. Let us introduce two Stein operators \mathcal{S} and $\tilde{\mathcal{S}}$ as follows:*

$$\begin{aligned} \mathcal{S}\phi(u) &= \langle DV(u), \phi(u) \rangle_{\mathcal{Y}} + \sum_{k=1}^{\infty} D_k \langle \phi(u), e_k \rangle_{\mathcal{Y}}, \quad \forall u \in \mathcal{X}, \\ \tilde{\mathcal{S}}\tilde{\phi}(\tilde{u}) &= \langle D_{\tilde{u}}V(T^{-1}\tilde{u}), \tilde{\phi}(\tilde{u}) \rangle_{\tilde{\mathcal{Y}}} + \sum_{k=1}^{\infty} D_{(\tilde{u})_k} \langle \tilde{\phi}(\tilde{u}), \tilde{e}_k \rangle_{\tilde{\mathcal{Y}}}, \quad \forall \tilde{u} \in \tilde{\mathcal{X}}, \end{aligned}$$

where $\{e_k\}_{k=1}^{\infty}$ and $\{\tilde{e}_k\}_{k=1}^{\infty}$ are orthonormal bases in \mathcal{Y} and $\tilde{\mathcal{Y}}$ respectively. Then, we have

$$(3.36) \quad \mathbb{E}_{u \sim \mu}[\mathcal{S}\phi(u)] = \mathbb{E}_{\tilde{u} \sim \tilde{\mu}}[\tilde{\mathcal{S}}\tilde{\phi}(\tilde{u})], \quad \text{with } \phi(u) := T^{-1}\tilde{\phi}(Tu).$$

Therefore, in the asymptotics of infinitesimal step size ($\epsilon \rightarrow 0^+$), running iSVG D with kernel \mathbf{K}_0 on $\tilde{\mu}$ is equivalent to running iSVG D on μ with the kernel $\mathbf{K}(u, u') = T^{-1}\mathbf{K}_0(Tu, Tu')(T^{-1})^*$, in the sense that the trajectory of these two SVG D can be mapped to each other by the map T (and its inverse).

Proof. Let us introduce a mapping defined by $u' = f(u) = u + \epsilon\phi(u)$, and then we denote $f_{\#}\mu$ as the probability measure $\mu \circ f^{-1}$. Let $\tilde{u}' \sim T_{\#}(f_{\#}\tilde{\mu})$ able to be obtained by

$$\begin{aligned} \tilde{u}' &= Tu' = T(u + \epsilon\phi(u)) = T(T^{-1}\tilde{u} + \epsilon\phi(T^{-1}\tilde{u})) \\ (3.37) \quad &= \tilde{u} + \epsilon T\phi(T^{-1}\tilde{u}) \\ &= \tilde{u} + \epsilon\tilde{\phi}(\tilde{u}), \end{aligned}$$

where we use the definition $\phi(u) = T^{-1}\tilde{\phi}(Tu)$ in (3.36). According to Theorem 3.1 in [32] and Theorem 3 in [48], we have $\mathbb{E}_{u^N \sim P_{\#}^N \mu}[\mathcal{S}^N \phi^N(u^N)] = \mathbb{E}_{u^N \sim P_{\#}^N \tilde{\mu}}[\tilde{\mathcal{S}}^N \tilde{\phi}^N(u^N)]$, where

$$\begin{aligned} \mathcal{S}^N \phi^N(u^N) &= \langle DV(u^N), \phi^N(u^N) \rangle_{\mathcal{Y}} + \sum_{k=1}^N D_k \langle \phi^N(u^N), e_k \rangle_{\mathcal{Y}}, \\ \tilde{\mathcal{S}}^N \tilde{\phi}^N(\tilde{u}^N) &= \langle D_{\tilde{u}^N} V(T^{-1}\tilde{u}^N), \tilde{\phi}^N(\tilde{u}^N) \rangle_{\tilde{\mathcal{Y}}} + \sum_{k=1}^N D_{(\tilde{u}^N)_k} \langle \tilde{\phi}^N(\tilde{u}^N), \tilde{e}_k \rangle_{\tilde{\mathcal{Y}}}. \end{aligned}$$

In the above formula, there is no Jacobian matrix term given by the variable transformation in $D_{\tilde{u}^N} V(T^{-1}\tilde{u}^N)$ since the Jacobian matrix does not depend on \tilde{u}^N for linear mapping (derivative is zero). Mimicking the proof given in Theorem 3.9, we can take $N \rightarrow \infty$ to obtain $\mathbb{E}_{u \sim \mu}[\mathcal{S}\phi(u)] = \mathbb{E}_{u \sim \tilde{\mu}}[\tilde{\mathcal{S}}\tilde{\phi}(u)]$. From Theorem 3.12, when $\tilde{\phi}$ is in $\tilde{\mathcal{F}}$ with kernel $\mathbf{K}_0(u, u')$, ϕ is in \mathcal{F} with kernel $\mathbf{K}(u, u')$. Therefore, maximizing $\mathbb{E}_{u \sim \mu}[\mathcal{S}\phi(u)]$ in \mathcal{F} is equivalent to $\mathbb{E}_{u \sim \tilde{\mu}}[\tilde{\mathcal{S}}\tilde{\phi}(u)]$ in $\tilde{\mathcal{F}}$. This suggests that the trajectory of iSVGd on $\tilde{\mu}^d$ with \mathbf{K}_0 and that on μ^d with \mathbf{K} are equivalent. Hence, the proof is completed. \square

Remark 3.14. Similar to the matrix-valued case [48], Theorem 3.13 suggests a conceptual procedure for constructing proper operator kernels to incorporate desirable preconditioning information. Different from the finite-dimensional case, at this moment, we only allow the map T is linear. For a nonlinear map, there will be a Jacobian matrix term in $\tilde{\mathcal{S}}^N \tilde{\phi}^N(\tilde{u}^N)$. It seems to be hard to analyze the limiting behavior of the Jacobian matrix related term. However, from the practical point of view, linear map seems to be enough since even in the finite-dimensional case nonlinear map will yield an unnatural algorithm [48].

In the last part of this subsection, we provide some examples of preconditioning operator that are frequently used in statistical inverse problems.

Fixed preconditioning operator: In Section 5 of [16], the authors considered Langevin equations with \mathcal{C}_0 as a preconditioner, and provided some interesting mathematical analysis related to pCN algorithm. In the Newton optimization method, we usually employ the inverse of the second-order derivative of the objective functional at the iterative points as the preconditioning operator [34]. Here, we consider a linear operator T that has similar properties as $\mathcal{C}_0^{-\frac{1-s}{2}}$. Specifically, we require

$$(3.38) \quad T \in \mathcal{L}(\mathcal{H}^{1-s}, \mathcal{H}) \cap \mathcal{L}(\mathcal{H}^{-1-s}, \mathcal{H}^{-2}).$$

Then, we specify the Hilbert space appearing in Theorem 3.12 as $\mathcal{X} = \mathcal{H}^{1-s}$, $\mathcal{Y} = \mathcal{H}^{-1-s}$, $\tilde{\mathcal{X}} = \mathcal{H}$, $\tilde{\mathcal{Y}} = \mathcal{H}^{-2}$ with $s \in [0, 1]$. For the kernel $\mathbf{K}_0(\cdot, \cdot) : \tilde{\mathcal{X}} \times \tilde{\mathcal{X}} \rightarrow \tilde{\mathcal{Y}}$, we assume that

$$(3.39) \quad \sup_{\tilde{u} \in \tilde{\mathcal{X}}} \|\mathbf{K}_0(\tilde{u}, \tilde{u})\|_{\mathcal{L}(\tilde{\mathcal{Y}})} < \infty.$$

Theorem 3.13 suggests to use a kernel of the form

$$(3.40) \quad \mathbf{K}(u, u') := T^{-1} \mathbf{K}_0(Tu, Tu')(T^{-1})^*$$

with $u, u' \in \mathcal{H}^{1-s}$. Obviously, the kernel \mathbf{K} given above satisfies

$$(3.41) \quad \sup_{u \in \mathcal{H}^{1-s}} \|T^{-1} \mathbf{K}_0(Tu, Tu)(T^{-1})^*\|_{\mathcal{L}(\mathcal{H}^{-1-s})} < \infty.$$

As an example, taking \mathbf{K}_0 to be the scalar-valued Gaussian RBF kernel composed with operator \mathcal{C}_0^s defined as follows:

$$(3.42) \quad \mathbf{K}_0(u, u') := \exp\left(-\frac{1}{h}\|T(u - u')\|_{\mathcal{H}}^2\right)\mathcal{C}_0^s.$$

Through this choice, we obtain

$$(3.43) \quad \mathbf{K}(u, u') = \exp\left(-\frac{1}{h}\|T(u - u')\|_{\mathcal{H}}^2\right)T^{-1}\mathcal{C}_0^s(T^{-1})^*,$$

where h is a bandwidth parameter. Define $\mathbf{K}_0^T(u, u') := \mathbf{K}_0(Tu, Tu')$. Let $\mathcal{P} := T^{-1}\mathcal{C}_0^s(T^{-1})^*$. Through simple calculations, we find that the iSVGd update direction of the kernel in (3.40) equals

$$(3.44) \quad \phi_{\mathbf{K}}^*(\cdot) = \mathcal{P}\mathbb{E}_{u \sim \mu}\left[\mathbf{K}_0^T(u, \cdot)(D\Phi(u) + \mathcal{C}_0^{-1}u) + \sum_{k=1}^{\infty} D_k \mathbf{K}_0^T(u, \cdot)e_k\right] = \mathcal{P}\phi_{\mathbf{K}_0^T}^*,$$

which is a linear transform of the iSVGd update direction of the kernel \mathbf{K}_0^T with the operator $T^{-1}\mathcal{C}_0^s(T^{-1})^*$.

Fixed preconditioning operator \mathcal{C}_0 : Choosing $T := \mathcal{C}_0^{-\frac{1-s}{2}}$, the condition (3.38) obviously holds true. Kernel \mathbf{K}_0 given in (3.42) has the following explicit form

$$(3.45) \quad \mathbf{K}_0(u, u') := \exp\left(-\frac{1}{h}\|\mathcal{C}_0^{-\frac{1-s}{2}}(u - u')\|_{\mathcal{H}}^2\right)\mathcal{C}_0^s,$$

and, in addition, kernel \mathbf{K} defined in (3.43) can be written as follows:

$$\mathbf{K}(u, u') = \exp\left(-\frac{1}{h}\|\mathcal{C}_0^{-\frac{1-s}{2}}(u - u')\|_{\mathcal{H}}^2\right)\mathcal{C}_0.$$

Now, operator \mathcal{P} used in (3.44) is just \mathcal{C}_0 . If there is only one particle, the iSVGd update direction is then reduced to $\phi_{\mathbf{K}}^*(\cdot) = \mathcal{C}_0(D\Phi(u) + \mathcal{C}_0^{-1}u)$.

Fixed preconditioning Hessian operator: For statistical inverse problems, the forward operator \mathcal{G} in (2.1) is usually nonlinear, e.g., forward map in inverse medium scattering problem [24, 25]. Around each particle u_i with $i = 1, 2, \dots, m$, the forward map can be approximated by

$$(3.46) \quad \mathcal{G}(u) \approx \mathcal{G}(u_i) + D\mathcal{G}(u_i)(u - u_i),$$

which is linear. Assume that the potential function Φ takes the following form $\Phi(u) = \frac{1}{2}\|\Sigma^{-1/2}(\mathcal{G}(u) - d)\|_{\ell^2}^2$, where Σ is a positive definite matrix. Using the approximate formula (3.46), we have

$$V(u) \approx \tilde{V}(u) := \frac{1}{2}\|\Sigma^{-1/2}(D\mathcal{G}(u_i)u - D\mathcal{G}(u_i)u_i + \mathcal{G}(u_i) - d)\|_{\ell^2}^2 + \frac{1}{2}\|\mathcal{C}_0^{-1/2}u\|_{\mathcal{H}}^2.$$

Through a simple calculation, we obtain $D^2\tilde{V}(u_i) = D\mathcal{G}(u_i)^*\Sigma^{-1}D\mathcal{G}(u_i) + \mathcal{C}_0^{-1}$. Along the research line of Newton-type optimization algorithm, we can take the linear transform $T = \mathcal{C}_0^{s/2}\left(\frac{1}{m}\sum_{i=1}^m(D\mathcal{G}(u_i)^*\Sigma^{-1}D\mathcal{G}(u_i) + \mathcal{C}_0^{-1})\right)^{1/2}$. If \mathcal{G} is a linear operator (e.g., examples in [23]), we can verify condition (3.38) easily. For specific nonlinear problems, we should employ the regularity properties of the forward equation, which is beyond the scope of the present work. We thus do not verify this condition in this paper and leave this issue to our future investigation. With this choice of T , the kernel (3.43) and the iSVGd update direction (3.44) can be easily written out. If there is only one particle, the iSVGd update direction can degenerate to the usual Newton update direction when evaluating MAP estimate.

Mixture preconditioning: Using fixed preconditioning operator, we can not specify different preconditioning operators for different particles. Inspired by mixture precondition studied in [48], we can present a practical approach to achieve point-wise preconditioning. The idea is to use a weighted combination of several linear preconditioning operators. This involves leveraging a set of anchor points $\{v_\ell\}_{\ell=1}^m$, each of which is associated with a preconditioning operator T_ℓ (e.g., $T_\ell = \mathcal{C}_0^{s/2}(D\mathcal{G}(v_\ell)^*\Sigma^{-1}D\mathcal{G}(v_\ell) + \mathcal{C}_0^{-1})^{1/2}$). In practice, the anchor points $\{v_\ell\}_{\ell=1}^m$ can be conveniently set to be the same as the particles $\{u_i\}_{i=1}^m$. We then construct a kernel by $\mathbf{K}(u, u') = \sum_{\ell=1}^m \mathbf{K}_\ell(u, u')w_\ell(u)w_\ell(u')$, where

$$(3.47) \quad \mathbf{K}_\ell(u, u') := T_\ell^{-1} \mathbf{K}_0(T_\ell u, T_\ell u')(T_\ell^{-1})^*,$$

and $w_\ell(u)$ is a positive scalar-valued function that decides the contribution of kernel \mathbf{K}_ℓ at point u . Here $w_\ell(u)$ should be viewed as a mixture probability, and hence should satisfy $\sum_{\ell=1}^m w_\ell(u) = 1$ for all u . In our empirical studies, we take

$$(3.48) \quad w_\ell(u) = \frac{\exp\left(-\frac{1}{2}\|T_\ell(u - v_\ell)\|_{\mathcal{H}}^2\right)}{\sum_{\ell'=1}^m \exp\left(-\frac{1}{2}\|T_{\ell'}(u - v_{\ell'})\|_{\mathcal{H}}^2\right)}.$$

In this way, each point u is mostly influenced by the anchor point closest to it, allowing us to apply different preconditioning for different points. In addition, the iSVGD update direction has the following form

$$(3.49) \quad \begin{aligned} \phi_{\mathbf{K}}^*(\cdot) = & \sum_{\ell=1}^m w_\ell(\cdot) \mathbb{E}_{u \sim \mu} \left[-w_\ell(u) \mathbf{K}_\ell(u, \cdot) (D\Phi(u) + \mathcal{C}_0^{-1}u) \right. \\ & \left. + \sum_{k=1}^{\infty} D_k(w_\ell(u) \mathbf{K}_\ell(u, \cdot) e_k) \right], \end{aligned}$$

which is a weighted sum of a number of iSVGD update directions with linear preconditioning operators. For highlighting the main ideas, we postpone the implementation details on (3.49) to the supplementary materials.

Remark 3.15. For the kernel defined above, we need the particles belonging to the Hilbert space \mathcal{H}^{1-s} . Intuitively, we may specify the parameter s equal to 0 based on the investigations conducted in the finite-dimensional theory [48]. However, when the parameter $s = 0$, each particle u_i belongs to \mathcal{H}^1 which is the Cameron-Martin space of the prior measure. By the classical Gaussian measure theory [15], we know that \mathcal{H}^1 has zero measure. This fact implies that all of the particles belong to a set with zero measure, which obviously leads to too concentrated particles conflicted with our purpose. The analysis shown here indicates that we should choose $s > 0$ to ensure the effectiveness of the SVGD sampling algorithm. Numerical illustrations of these facts are given in Section 4 for an inverse problem governed by a Helmholtz equation.

4. APPLICATIONS

The proposed framework is valid for Bayesian inverse problems governed by any systems of forward PDEs. In this section we will illustrate the use of the framework on a frequency domain acoustic wave equation in the form of the Helmholtz equation

as follows:

$$(4.1) \quad \begin{aligned} -\Delta w - e^{2u}w &= 0 \text{ in } \Omega, \\ \frac{\partial w}{\partial \mathbf{n}} &= g \text{ in } \partial\Omega, \end{aligned}$$

where w is the acoustic field, u is the logarithm of the distributed wave number field on Ω (Ω is a bounded domain), \mathbf{n} is the unit outward normal on $\partial\Omega$, and g is the prescribed Neumann source on the boundary. This model has been investigated during the investigations of a randomized maximum a posteriori (rMAP) method [34]. For the implementations of the iSVGd approach, it is essential to compute the gradient and Hessian through the adjoint method, which is illustrated in Section 6 of [34]. For the reader's convenience, we provide explicit forms of adjoint, incremental forward, and incremental adjoint equations in the supplementary materials.

4.1. Basic settings and finite-element discretization. For practical problems, we choose Ω to be a rectangular domain $\Omega = [0, 1]^2 \subset \mathbb{R}^2$, set $\mathcal{H} = L^2(\Omega)$, and consider the prior measure $\mu_0 = \mathcal{N}(u_0, \mathcal{C}_0)$ with mean function u_0 and covariance operator $\mathcal{C}_0 := A^{-2}$, where $A = \alpha(I - \Delta)$ ($\alpha > 0$) with the domain of definition of A defined as $D(A) := \left\{ u \in H^2(\Omega) : \frac{\partial u}{\partial \mathbf{n}} = 0 \text{ on } \partial\Omega \right\}$. Here, $H^2(\Omega)$ is the usual Sobolev space. Assume that the mean function u_0 resides in the Cameron-Martin space of μ_0 .

Let \mathcal{F} be the solution mapping that maps the parameter u to the solution of the equation (4.1), and \mathcal{M} be the measurement operator defined as $\mathbf{d} = \mathcal{M}(w) = (w(x_1), w(x_2), \dots, w(x_{N_d}))^T$, with $x_i \in \partial\Omega$ for $i = 1, \dots, N_d$. Now, the forward map can be defined as $\mathcal{G} := \mathcal{M} \circ \mathcal{F}$, and the problem can be written in the abstract form $\mathbf{d} = \mathcal{G}(u) + \epsilon$ with $\epsilon \sim \mathcal{N}(0, \sigma^2 \text{Id})$. Here, we will not illustrate the conditions required by the Bayesian inverse method and the conditions employed in the previous section since this is not the main focus of the present work. However, based on the previous analysis of Helmholtz equations shown in [24, 25], we believe that the required conditions can be verified, which will be investigated in our future research.

For finite-dimensional approximations, we consider a finite-dimensional subspace V_h of $L^2(\Omega)$ originating from element discretization with continuous Lagrange basis function $\{\phi_j\}_{j=1}^n$, which correspond to the nodal points $\{x_j\}_{j=1}^n$, such that $\phi_j(x_i) = \delta_{ij}$ for $i, j \in \{1, \dots, n\}$. Instead of statistically inferring parameter functions $u \in L^2(\Omega)$, we perform this task on the approximation $u_h = \sum_{j=1}^n u_j \phi_j \in V_h$. Under this finite-dimensional approximation, we can employ the numerical method provided in [4] to discretize the prior, and construct finite-dimensional approximations of the Gaussian approximation of the posterior measure. Based on our analysis in Subsection 3.3, we need to calculate the fractional powers of the operator \mathcal{C}_0 . Here, we employ the matrix transfer technique (MTT) which has been discussed in detail in [6]. The main ideas of MTT is to indirectly discretize a fractional Laplacian using a discretization of the standard Laplacian. As discussed in [4], we will meet the operator $M^{1/2}$ with

$$(4.2) \quad M = (M_{ij})_{i,j=1}^n \quad \text{and} \quad M_{ij} = \int_{\Omega} \phi_i(x) \phi_j(x) dx, \quad i, j \in \{1, \dots, n\}.$$

In our numerical implementations, the matrix $M^{1/2}$ is just simply approximated by a diagonal matrix $\text{diag}(M_{11}^{1/2}, \dots, M_{nn}^{1/2})$.

At last, it should be indicated that the finite element discretization is implemented by employing the open software FEniCS (Version 2019.1.0) [33]. All programs were run on a personal computer with Intel(R) Core(TM) i7-7700 at 3.60 GHz (CPU), 32 GB (memory), and Ubuntu 18.04.2 LTS (OS).

4.2. Numerical results. Since the experiments aim at testing algorithms rather than demonstrating Bayesian modeling, we conveniently fix the noise level for all of the numerical experiments to be 1%. We will compare iSVGDMPO with preconditioned Crank-Nicolson (pCN) sampling algorithm [16] and randomized maximum a posteriori (rMAP) algorithm [49]. Since rMAP sampling algorithm is not accurate for nonlinear problems, we choose $\alpha = 0.5$ in the prior probability measure, which makes the non-linearity dominated. For the initial particles of iSVGDMPO, we generate them from a probability measure constructed according to the methods provided in [4]. The method given in [4], in our opinion, can be seen as the Gaussian approximation (GA) of the posterior measure [2].

For the current inverse problems, it is necessary for employing optimization methods with preconditioning operators, e.g., Newton-conjugate gradient method. For conciseness, we present a detailed comparison in the supplementary materials, which illustrate the necessity for introducing preconditioning operators.

In the following, we compare the performance of iSVGDMPO equipped with mixture preconditioning operator (iSVGDMPO) with those obtained by pCN and rMAP sampling algorithms. As illustrated in Remark 3.15, the parameter s should be set larger than zero. Intuitively, the particles should belong to a space with probability approximately equal to one under the prior measure μ_0 . According to the Gaussian measure theory [15], we should take $s > 0.5$ since $\mu_0(\mathcal{H}^{1-s}) = 1$ for any $s > 0.5$. Considering that the posterior measure is usually concentrated on a small set of the support of the prior measure, the parameter s should be taken slightly smaller than 0.5. Thus, we prefer to set $s = 0.3$ or 0.4 for practical problems. Usually, the initial particles are scattered, and the variances of the initial particles are larger than the final particles obtained by iSVGDMPO or iSVGDMPO. We then design the following empirical strategies for changing s adaptively:

$$(4.3) \quad s = -0.5 \frac{\|\text{var}\|_{\ell^2}}{\|\text{var}_0\|_{\ell^2}} + 0.5,$$

where var is the current estimated variance, var_0 is the estimated variance of the initial particles, and $\|\cdot\|_{\ell^2}$ is the usual ℓ^2 -norm. Obviously, for the initial particles, we have $s = 0$. The particles are forced to be concentrated. When the variance is reduced, the parameter s will approach 0.5 to ensure that the particles are scattered (not concentrated on a set with zero measure). Since pCN is a dimension independent MCMC type sampling algorithm, we take the results obtained by pCN as the baseline (accurate estimate). In order to make sure that the pCN algorithm offers an accurate estimate, we iterate 5×10^5 steps and withdraw the first 10^5 samples. We try several different step-sizes and plot the traces of some parameters, and then pick the most reliable one as our final estimate.

In Figure 1, we show the estimated variances obtained by iSVGDMPO (blue solid line), rMAP (green dotted line) and pCN (orange dashed line) sampling algorithms. Specifically, we show the estimated variances of iSVGDMPO when $s = 0$ and $s = 0.4$ on the left panel and in the middle panel, respectively. On the right

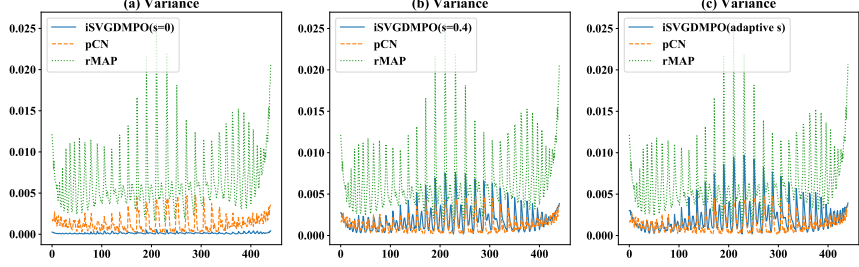


FIGURE 1. Compare variances estimated by pCN, rMAP, iSVGDMPO with different s . (a): variances estimated by pCN, rMAP, and iSVGDMPO ($s = 0$); (b): variances estimated by pCN, rMAP, and iSVGDMPO ($s = 0.4$); (c): variances estimated by pCN, rMAP, and iSVGDMPO (adaptive s).

panel, we exhibit the estimated variances when the empirical adaptive strategy (4.3) is employed. As expected, the estimated variances are too small when $s = 0$, which indicates that the particles are concentrated on a small set (theoretically on a set with zero measure). Choosing $s = 0.4$ or using the empirical strategy, we obtain similar estimates, which is more similar to the baseline obtained by pCN compared with the estimates obtained by rMAP. In the following numerical experiments, we use the empirical adaptive strategy to specify the parameter s . In the supplementary materials, we provide three videos to exhibit the dynamic changing procedure of the estimated variances. In addition, the update perturbation with and without repulsive force term (term on the second line of (3.49)) are exhibited. These videos can further illustrate our findings shown here. And we can see that the repulsive force terms indeed take effect to prevent particles concentrated.

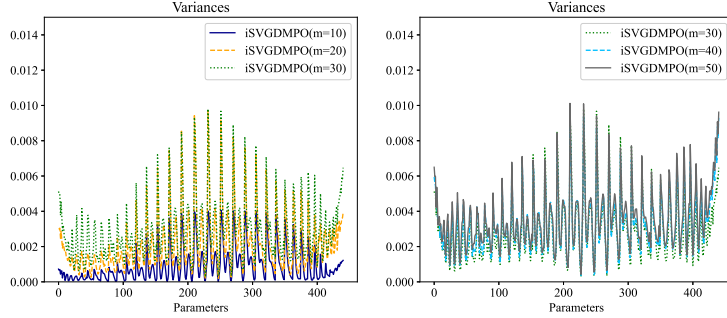


FIGURE 2. Compare variances estimated by iSVGDMPO when $s = 10, 20, 30, 40, 50$.

Apart from the parameter s , how many samples should be taken to guarantee a stable variance estimation is important for using iSVGDMPO. When the particle number is too small, we cannot obtain reliable estimates. On the contrary, the computational complexity will increase when the particle number increases. In Figure 2, we show the estimated variances when particle number equals to 10, 20, 30, 40, and 50. Let us denote m be the number of samples. On the left panel in Figure 2, we show the results obtained when $m = 10, 20, 30$. Obviously, when

$m = 10$, the estimated variances are significantly smaller than those obtained when $m = 20, 30$. On the right panel in Figure 2, we find that the estimated variances are similar when $m = 30, 40, 50$. Hence, it is enough for our numerical examples to take $m = 20$ or 30 , which inclines to attain a fine balance between efficiency and accuracy.

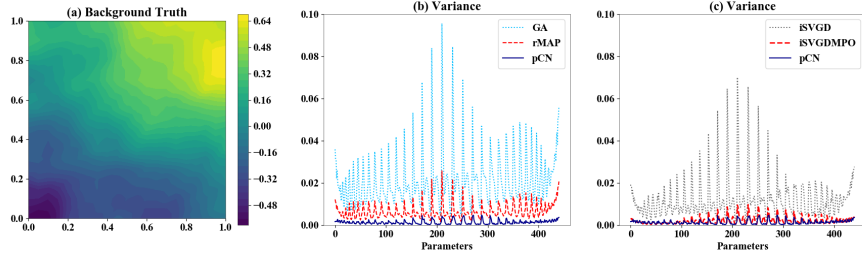


FIGURE 3. Background truth and estimated variances by pCN, GA, rMAP, iSVGd, and iSVGDMPO. (a): background truth; (b): estimated variances by pCN(solid dark-blue line), GA(dotted light-blue line), and rMAP(dashed red line); (c): estimated variances by pCN(solid dark-blue line), iSVGd(dotted gray line), and iSVGDMPO with adaptive s (dashed red line).

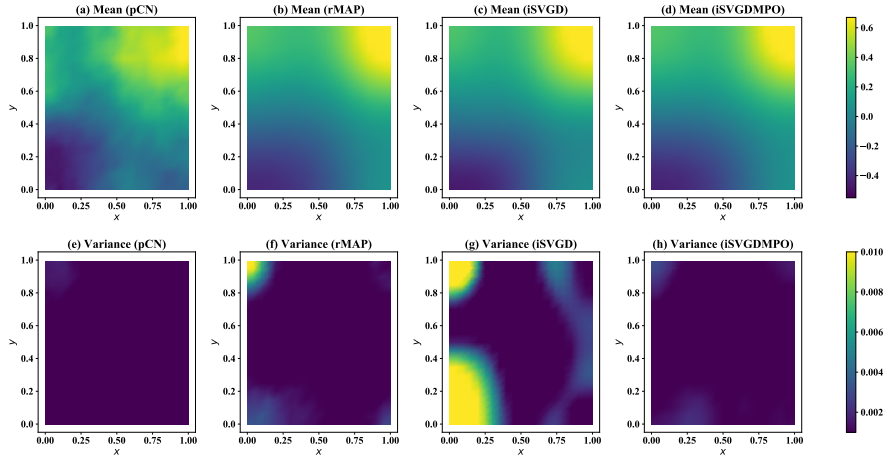


FIGURE 4. Estimated mean functions and variances by pCN, rMAP, iSVGd, and iSVGDMPO. (a): estimated mean function by pCN; (b): estimated mean function by rMAP; (c): estimated mean function by iSVGd; (d): estimated mean function by iSVGDMPO; (e): estimated variance by pCN; (f): estimated variance by rMAP; (g): estimated variance by iSVGd; (h): estimated variance by iSVGDMPO.

Now, we specify the sampling number $m = 20$ and set the parameter s by the proposed empirical strategy (4.3). In Figure 3, we demonstrate the background truth and the estimated variances obtained by pCN, GA, rMAP, iSVGd, and

iSVGDMPO, respectively. It should be mentioned that the iterative numbers of iSVGDMPO and iSVGDMPO are set to be 2000 and 40, respectively. From (b) and (c) in Figure 3, we clearly find that the estimated variance of iSVGDMPO is closer to the baseline than that obtained by GA and rMAP. GA provides relatively not satisfactory estimate. Although the iterative number of iSVGDMPO is 2000, it still cannot make the particles well concentrated, which might possibly be due to the ineffectiveness of the gradient descent in this numerical example. In Figure 4, we compare the estimated mean and variance functions calculated by pCN, rMAP, iSVGDMPO, and iSVGDMPO. It can be evidently observed that the mean functions obtained by rMAP, iSVGDMPO, and iSVGDMPO are similar, which are slightly smoother than the one obtained by the pCN algorithm. From the second line in Figure 4, we can see that iSVGDMPO provides a more reliable estimate of the variances than those obtained by the iSVGDMPO and rMAP algorithms.

5. CONCLUSION

In this paper, we have investigated the approximate sampling algorithm for the infinite-dimensional Bayesian approach to inverse problems. Specifically, we have defined the Stein operator on Hilbert space and proved that the introduced Stein operator is indeed the limit of the finite-dimensional version. Besides, we have constructed the update perturbation of SVGDMPO on infinite-dimensional space (called iSVGDMPO) by using properties of operator-valued RKHS. For accelerating the convergence speed of iSVGDMPO, we have further investigated the change of variables formula and introduced preconditioning operator, which yields more efficient algorithms. As examples, we present fixed preconditioning operator and mixture preconditioning operator. Then, we have calculated the explicit form of the update directions for iSVGDMPO with mixture preconditioning operator (iSVGDMPO). Finally, we have applied the constructed algorithms to an inverse problem governed by a Helmholtz equation. Through comparisons with pCN and rMAP sampling algorithms, it can be substantiated that the proposed algorithms can generate accurate estimates efficiently.

We have investigated iSVGDMPO rigorously through a careful study of the limiting behavior of the finite-dimensional objects. Through this study, we have constructed an infinite-dimensional version of the approach given in [48]. It should be noted that our results not only provide an infinite-dimensional version but also indicate that an intuitive trivial generalization of algorithms given in [48] may not be suitable since particles will belong to a set with zero measure. Our theoretical and numerical results all reflect that it is necessary to introduce the parameter s in Assumption 3.8, which has not been raised to be concerned in previous investigations.

6. SUPPLEMENTARY MATERIAL

In this supplementary material, we introduce more useful examples and demonstrating more illustration details, which will be beneficial for easier understandings of the main text.

6.1. Example of kernel satisfy assumption (27) in Theorem 11. In this section, let us give an example of the kernel that satisfies assumption (27) given in Theorem 11 of the main text. For reader's convenience, let us recall that assumption

(31) states the following quantity

$$(6.1) \quad \mathbb{E}_{u \sim \mu} \left[D_{u'} \mathbf{K}(u, u') \mathcal{C}_0^{-1/2} g + \sum_{k=1}^{\infty} D_k D_{u'} \mathbf{K}(u, u') e_k \right]$$

belongs to $\mathcal{L}_1(\mathcal{X}, \mathcal{Y})$ for each $u' \in \mathcal{X}$ and $g \in \mathcal{H}^{-s}$.

Now, Let us take $\mathbf{K}(u, u') = K(u, u') \text{Id}$ with

$$K(u, u') = \exp \left(-\frac{1}{h} \|u - u'\|_{\mathcal{X}}^2 \right)$$

to be a scalar-valued kernel. For this special kernel, we have

$$D_{u'} \mathbf{K}(u, u') = -\frac{1}{h} \langle u - u', \cdot \rangle_{\mathcal{X}} K(u, u'),$$

$$D_k D_{u'} \mathbf{K}(u, u') e_k = \frac{1}{h^2} (u_k - u'_k) \langle u - u', \cdot \rangle_{\mathcal{X}} K(u, u') e_k.$$

Let $\{\varphi_j\}_{j=1}^{\infty}$ be an orthonormal basis of \mathcal{X} , and recall that $\{e_j\}_{j=1}^{\infty}$ represents an orthonormal basis of \mathcal{Y} . Plugging the above formula into (6.1), we find that

$$\sum_{j=1}^{\infty} \langle \mathbb{E}_{u \sim \mu} \left[D_{u'} \mathbf{K}(u, u') \mathcal{C}_0^{-1/2} g + \sum_{k=1}^{\infty} D_k D_{u'} \mathbf{K}(u, u') e_k \right] \varphi_j, e_j \rangle = \mathbb{E}_{u \sim \mu} \{ \text{I} + \text{II} \}$$

with

$$\text{I} = -\frac{1}{h} \sum_{j=1}^{\infty} \langle \langle u - u', \varphi_j \rangle_{\mathcal{X}} K(u, u') \mathcal{C}_0^{-1/2} g, e_j \rangle_{\mathcal{Y}},$$

$$\text{II} = \frac{1}{h^2} \sum_{j=1}^{\infty} \langle \sum_{k=1}^{\infty} (u_k - u'_k) e_k \langle u - u', \varphi_j \rangle_{\mathcal{X}}, e_j \rangle_{\mathcal{Y}} K(u, u').$$

For term I, we have

$$(6.2) \quad \begin{aligned} \text{I} &\leq \frac{1}{h} K(u, u') \left(\sum_{j=1}^{\infty} \langle u - u', \varphi_j \rangle_{\mathcal{X}}^2 \right)^{1/2} \left(\sum_{j=1}^{\infty} \langle \mathcal{C}_0^{-1/2} g, e_j \rangle \right)^{1/2} \\ &\leq \frac{C}{h} K(u, u') \|u - u'\|_{\mathcal{X}} \|\mathcal{C}_0^{-1/2} g\|_{\mathcal{Y}} \\ &\leq \frac{C}{h} K(u, u') \|u - u'\|_{\mathcal{X}} \|g\|_{\mathcal{H}^{-s}} < \infty. \end{aligned}$$

For term II, we have

$$(6.3) \quad \begin{aligned} \text{II} &\leq \frac{1}{h^2} K(u, u') \sum_{j=1}^{\infty} \langle u - u', \varphi_j \rangle_{\mathcal{X}} \langle (u_j - u'_j) e_j, e_j \rangle_{\mathcal{Y}} \\ &\leq \frac{1}{h^2} K(u, u') \left(\sum_{j=1}^{\infty} \langle u - u', \varphi_j \rangle_{\mathcal{X}}^2 \right)^{1/2} \left(\sum_{j=1}^{\infty} (u_j - u'_j)^2 \right)^{1/2} \\ &\leq \frac{1}{h^2} K(u, u') \|u - u'\|_{\mathcal{X}}^2 < \infty. \end{aligned}$$

Combining estimates (6.2) and (6.3), we obtain

$$(6.4) \quad \sum_{j=1}^{\infty} \langle \mathbb{E}_{u \sim \mu} \left[D_{u'} \mathbf{K}(u, u') \mathcal{C}_0^{-1/2} g + \sum_{k=1}^{\infty} D_k D_{u'} \mathbf{K}(u, u') e_k \right] \varphi_j, e_j \rangle < \infty,$$

which reflects that (6.1) belongs to $\mathcal{L}_1(\mathcal{X}, \mathcal{Y})$. Taking $\mathcal{X} = \mathcal{H}^1, \mathcal{Y} = \mathcal{H}^{-1}, s = 0$, and projecting all of the quantities to \mathcal{X}^N , we can then recover the finite-dimensional SVGD approach as reviewed in Section 2 of the main text.

6.2. Implementation details for mixture preconditioning. At the end of Subsection 3.3, we present the mixture preconditioning operators, which have the ability to specify different preconditioning operators for different particles. In the following, we provide more implementation details.

In practice, we approximate the expectation $\mathbb{E}_{u \sim \mu}$ by empirical mean of particles $\{u_i\}_{i=1}^m$. Hence, the formula (57) in the main text can be reduced to

$$(6.5) \quad \phi_{\mathbf{K}}^*(\cdot) = \sum_{\ell=1}^m w_{\ell}(\cdot) \sum_{j=1}^m \left[-w_{\ell}(u_j) \mathbf{K}_{\ell}(u_j, \cdot) (D_{u_j} \Phi(u_j) + \mathcal{C}_0^{-1} u_j) + \sum_{k=1}^{\infty} D_k(w_{\ell}(u_j) \mathbf{K}_{\ell}(u_j, \cdot) e_k) \right].$$

Taking \mathbf{K}_{ℓ} defined in (55) specified in the main text with

$$T_{\ell} = \mathcal{C}_0^{s/2} (D\mathcal{G}(u_{\ell})^* \Sigma^{-1} D\mathcal{G}(u_{\ell}) + \mathcal{C}_0^{-1})^{1/2},$$

we find that

$$\begin{aligned} & \mathbf{K}_{\ell}(u_j, \cdot) (D_{u_j} \Phi(u_j) + \mathcal{C}_0^{-1} u_j) \\ &= (D\mathcal{G}(u_{\ell})^* \Sigma^{-1} D\mathcal{G}(u_{\ell}) + \mathcal{C}_0^{-1})^{-1} (D_{u_j} \Phi(u_j) + \mathcal{C}_0^{-1} u_j) \exp\left(-\frac{1}{h} \|T_{\ell}(u_j - \cdot)\|_{\mathcal{H}}^2\right). \end{aligned}$$

For the term $D_k(w_{\ell}(u_j) \mathbf{K}_{\ell}(u_j, \cdot) e_k)$, we easily have

$$(6.6) \quad D_k(w_{\ell}(u_j) \mathbf{K}_{\ell}(u_j, \cdot) e_k) = D_k w_{\ell}(u_j) \mathbf{K}_{\ell}(u_j, \cdot) e_k + w_{\ell}(u_j) D_k \mathbf{K}_{\ell}(u_j, \cdot) e_k.$$

For the first term, we have

$$(6.7) \quad \begin{aligned} D_k w_{\ell}(u_j) \mathbf{K}_{\ell}(u_j, \cdot) e_k &= -\langle T_{\ell}(u_j - u_{\ell}), T_{\ell} \varphi_k \rangle w_{\ell}(u_j) \mathbf{K}_{\ell}(u_j, \cdot) e_k \\ &\quad - J_k w_{\ell}(u_j) \mathbf{K}_{\ell}(u_j, \cdot) e_k \end{aligned}$$

with

$$(6.8) \quad J_k = \frac{\sum_{\ell'=1}^m \langle T_{\ell}(u_j - u_{\ell'}), T_{\ell} \varphi_k \rangle \exp\left(-\frac{1}{2} \|T_{\ell'}(u_j - u_{\ell'})\|_{\mathcal{H}}^2\right)}{\sum_{\ell'=1}^m \exp\left(-\frac{1}{2} \|T_{\ell'}(u_j - u_{\ell'})\|_{\mathcal{H}}^2\right)}.$$

For the second term, we have

$$(6.9) \quad w_{\ell}(u_j) D_k \mathbf{K}_{\ell}(u_j, \cdot) e_k = -\frac{2}{h} w_{\ell}(u_j) \langle T_{\ell}(u_j - \cdot), T_{\ell} \varphi_k \rangle \mathbf{K}_{\ell}(u_j, \cdot) e_k.$$

Combining (6.7), (6.8) and (6.9), we obtain

$$(6.10) \quad \begin{aligned} \sum_{k=1}^{\infty} D_k(w_{\ell}(u_j) \mathbf{K}_{\ell}(u_j, \cdot) e_k) &= -\frac{2}{h} w_{\ell}(u_j) \sum_{k=1}^{\infty} \langle T_{\ell}(u_j - \cdot), T_{\ell} \varphi_k \rangle \mathbf{K}_{\ell}(u_j, \cdot) e_k \\ &\quad - w_{\ell}(u_j) \sum_{k=1}^{\infty} \langle T_{\ell}(u_j - u_{\ell}), T_{\ell} \varphi_k \rangle \mathbf{K}_{\ell}(u_j, \cdot) e_k \\ &\quad - w_{\ell}(u_j) \sum_{\ell'=1}^m \sum_{k=1}^{\infty} \langle T_{\ell'}(u_j - \cdot), T_{\ell'} \varphi_k \rangle \mathbf{K}_{\ell}(u_j, \cdot) e_k M_{\ell'}, \end{aligned}$$

where

$$(6.11) \quad M_{\ell'} = \frac{\exp\left(-\frac{1}{2}\|T_{\ell'}(u_j - u_{\ell'})\|_{\mathcal{H}}^2\right)}{\sum_{\ell''=1}^m \exp\left(-\frac{1}{2}\|T_{\ell''}(u_j - u_{\ell''})\|_{\mathcal{H}}^2\right)}.$$

For specific examples, we can find the explicit form of the following term:

$$(6.12) \quad \sum_{k=1}^{\infty} \langle T_{\ell}(u_j - \cdot), T_{\ell}\varphi_k \rangle \mathbf{K}_{\ell}(u_j, \cdot) e_k.$$

For example, we take \mathcal{X} , \mathcal{Y} , $\tilde{\mathcal{X}}$, and $\tilde{\mathcal{Y}}$ as in the fixed precondition case and specify \mathbf{K}_{ℓ} as in (51) of the main text with T replaced by T_{ℓ} . Then, we have

$$(6.13) \quad \begin{aligned} & \sum_{k=1}^{\infty} \langle T_{\ell}(u_j - \cdot), T_{\ell}\varphi_k \rangle \mathbf{K}_{\ell}(u_j, \cdot) e_k \\ &= \exp\left(-\frac{1}{h}\|T_{\ell}(u_j - \cdot)\|_{\mathcal{H}}^2\right) T_{\ell}^{-1} \mathcal{C}_0^s (T_{\ell}^{-1})^* \mathcal{C}_0^{-s} T_{\ell}^* T_{\ell}(u_j - \cdot). \end{aligned}$$

Hence, we actually need not to calculate the orthonormal basis $\{e_k\}_{k=1}^{\infty}$ and $\{\varphi_i\}_{i=1}^{\infty}$ in spaces \mathcal{Y} and \mathcal{X} explicitly during the implementations.

6.3. Explicit forms of adjoint, incremental forward and adjoint equations.

As explained in [49], we need adjoint, incremental forward, and incremental adjoint equations to compute gradient and Hessian-vector product efficiently. For the functional V , the gradient $DV(u)$ acting in any direction \tilde{u} is given by

$$\langle DV(u), \tilde{u} \rangle = -2 \int_{\Omega} \tilde{u} e^{2u} w \tau dx,$$

where the adjoint state τ satisfies the adjoint equation

$$\begin{aligned} -\Delta \tau - e^{2u} \tau &= -\frac{1}{\sigma^2} \sum_{j=1}^{N_d} (w - d_j) \delta(x - x_j) \text{ in } \Omega, \\ \frac{\partial \tau}{\partial \mathbf{n}} &= 0 \text{ on } \partial\Omega, \end{aligned}$$

where σ is the standard deviation of the noises, e.g., $\epsilon \sim \mathcal{N}(0, \sigma^2 \text{Id})$.

On the other hand, the Gauss-Newton Hessian acting in directions \tilde{u} and $\tilde{\tilde{u}}$ reads

$$\langle \langle D^2 V(u), \tilde{u} \rangle, \tilde{\tilde{u}} \rangle = -2 \int_{\Omega} \tilde{u} e^{2u} w \tilde{\tilde{u}} dx,$$

where the incremental forward state \tilde{w} satisfies

$$\begin{aligned} -\Delta \tilde{w} - e^{2u} \tilde{w} &= 2\tilde{u} e^{2u} w \text{ in } \Omega, \\ \frac{\partial \tilde{w}}{\partial \mathbf{n}} &= 0 \text{ on } \partial\Omega, \end{aligned}$$

and the incremental adjoint state $\tilde{\tau}$ obeys the following incremental adjoint equation:

$$\begin{aligned} -\Delta \tilde{\tau} - e^{2u} \tilde{\tau} &= -\frac{1}{\sigma^2} \sum_{j=1}^{N_d} \tilde{w} \delta(x - x_j) \text{ in } \Omega, \\ \frac{\partial \tilde{\tau}}{\partial \mathbf{n}} &= 0 \text{ on } \partial\Omega. \end{aligned}$$

6.4. Comparison between gradient descent and Newton type methods.

In this section, we focus on the explicit numerical example of Helmholtz equation studied in Section 4 of the main text. Specifically, we present the MAP estimate obtained by gradient descent (GD) and an inexact matrix-free Newton-conjugate gradient (IMFNCG) algorithm, which is suitable for computing large-scale inverse problems. For more details about the IMFNCG algorithm, we refer to [4, 49] and references therein. The step length of GD and IMFNCG are determined by the Armijo line search, and the initial guess is set to be a zero function.

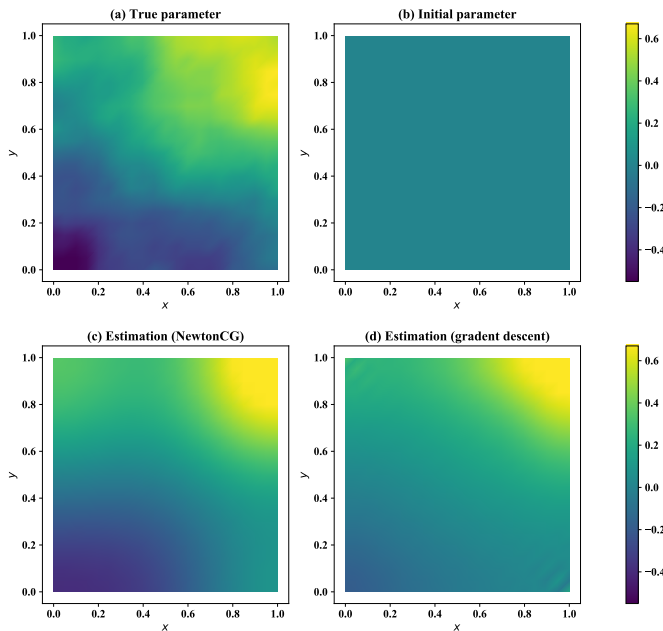


FIGURE 5. Comparison between the estimation results obtained by the gradient descent (GD) and IMFNCG algorithms. (a): the background truth; (b): the initial guess of the parameter; (c): the MAP estimate obtained by the IMFNCG algorithm with 7 steps; (d): the MAP estimate obtained by the GD algorithm with 1000 steps.

Numerical results are depicted in Figure 5. On the top left, we show the background truth function u . On the top right, we show the initial zero function. In the second row, we show the MAP estimates obtained by IMFNCG and GD algorithms, respectively. Obviously, the IMFNCG algorithm with only 7 steps of iteration achieves a reasonable estimate. However, the GD algorithm with Armijo line search cannot provide an estimate as accurate as the estimate given by IMFNCG even after 1000 iterative steps. The iSVGd sampling algorithm with no preconditioning can be reduced to GD algorithm when only one particle is considered. Hence, it is expected that the iSVGd sampling algorithm cannot work well since particles can hardly concentrate due to the inefficiency of the optimization procedure. These results verify that it is necessary to introduce iSVGd with preconditioning operator to enhance the optimization procedure. Only with an efficient optimization

procedure, the concentrate force (i.e., the first term in the bracket of (40) in the main text) and the repulsive force (i.e., the second term in the bracket of (40) in the main text) can sufficiently play their roles to provide accurate samplings.

ACKNOWLEDGMENTS

This work was partially supported by the NSFC under the grants No. 11871392.

REFERENCES

- [1] S. Arridge, P. Maass, O. Öktem, and C.-B. Schönlieb. Solving inverse problems using data-driven models. *Acta Numer.*, 28(1):1–174, 2019.
- [2] C. M. Bishop. *Pattern Recognition and Machine Learning*. Springer-Verlag, New York, NY, USA, 2006.
- [3] C. Brouard, M. Szafranski, and F. d’Alché Buc. Input output kernel regression: supervised and semi-supervised structured output prediction with operator-valued kernels. *J. Mach. Learn. Res.*, 17:1–48, 2016.
- [4] T. Bui-Thanh, O. Ghattas, J. Martin, and G. Stadler. A computational framework for infinite-dimensional Bayesian inverse problems part I: The linearized case, with application to global seismic inversion. *SIAM J. Sci. Comput.*, 35(6):A2494–A2523, 2013.
- [5] M. Burger and F. Lucka. Maximum a posteriori estimates in linear inverse problems with log-concave priors are proper Bayes estimators. *Inverse Probl.*, 30(11):114004, 2014.
- [6] T. But-Thanh and Q. P. Nguyen. FEM-based discretization-invariant MCMC methods for PDE-constrained Bayesian inverse problems. *Inverse Probl. Imag.*, 10(4):943–975, 2016.
- [7] C. Carmeli, E. D. Vito, and A. Toigo. Vector valued reproducing kernel Hilbert spaces of integrable functions and Mercer theorem. *Anal. Appl.*, 4(4):377–408, 2006.
- [8] C. Carmeli, E. D. Vito, and A. Toigo. Vector-valued reproducing kernel Hilbert spaces and universality. *Anal. Appl.*, 8(1):19–61, 2010.
- [9] E. D. C. Carvalho, R. Clark, A. Nicastró, and P. H. J. Kelly. Scalable uncertainty for computer vision with functional variational inference. In *CVPR*, pages 12003–12013, 2020.
- [10] P. Chen and O. Ghattas. Stein variational reduced basis Bayesian inversion. arXiv:2002.10924, 2020.
- [11] P. Chen, K. Wu, J. Chen, T. O’Leary-Roseberry, and O. Ghattas. Projected Stein variational Newton: a fast and scalable Bayesian inference method in high dimensions. In *NeurIPS*, volume 32, 2019.
- [12] S. L. Cotter, G. O. Roberts, A. M. Stuart, and D. White. MCMC methods for functions: modifying old algorithms to make them faster. *Stat. Sci.*, 28(3):424–446, 2013.
- [13] Simon L Cotter, Massoumeh Dashti, James Cooper Robinson, and Andrew M Stuart. Bayesian inverse problems for functions and applications to fluid mechanics. *Inverse Probl.*, 25(11):115008, 2009.
- [14] T. Cui, K. J. H. Law, and Y. M. Marzouk. Dimension-independent likelihood-informed MCMC. *J. Comput. Phys.*, 304:109–137, 2016.
- [15] G. DaPrato and J. Zabczyk. *Stochastic Equations in Infinite Dimensions*. Cambridge University Press, Cambridge, 1992.
- [16] M. Dashti and A. M. Stuart. The Bayesian approach to inverse problems. *Handbook of Uncertainty Quantification*, pages 311–428, 2017.
- [17] G. Detommaso, T. Cui, A. Spantini, and Y. Marzouk. A Stein variational Newton method. In *NeurIPS*, volume 32, 2018.
- [18] H. W. Engl, M. Hanke, and A. Neubauer. *Regularization of Inverse Problems*. Springer, Netherlands, 1996.
- [19] Z. Feng and J. Li. An adaptive independence sampler MCMC algorithm for Bayesian inferences of functions. *SIAM J. Sci. Comput.*, 40(3):A1310–A1321, 2018.
- [20] A. Fichtner. *Full Seismic Waveform Modelling and Inversion*. Springer, New York, 2011.
- [21] N. Guha, X. Wu, Y. Efendiev, B. Jin, and B. K. Mallick. A variational Bayesian approach for inverse problems with skew-t error distribution. *J. Comput. Phys.*, 301:377–393, 2015.
- [22] T. Helin and M. Burger. Maximum a posteriori probability estimates in infinite-dimensional Bayesian inverse problems. *Inverse Probl.*, 31(8):085009, 2015.

- [23] J. Jia, J. Peng, and J. Gao. Posterior contraction for empirical Bayesian approach to inverse problems under non-diagonal assumption. *Inverse Probl. Imag.*, 15(2):201–228, 2020.
- [24] J. Jia, B. Wu, J. Peng, and J. Gao. Recursive linearization method for inverse medium scattering problems with complex mixture Gaussian error learning. *Inverse Probl.*, 35(7):075003, 2019.
- [25] J. Jia, S. Yue, J. Peng, and J. Gao. Infinite-dimensional Bayesian approach for inverse scattering problems of a fractional Helmholtz equation. *J. Funct. Anal.*, 275(9):2299–2332, 2018.
- [26] J. Jia, Q. Zhao, D. Meng, and Y. Leung. Variational Bayes’ method for functions with applications to some inverse problems. *SIAM J. Sci. Comput.*, 43(1):A355–A383, 2021.
- [27] B. Jin. A variational Bayesian method to inverse problems with implusive noise. *J. Comput. Phys.*, 231:423–435, 2012.
- [28] B. Jin and J. Zou. Hierarchical Bayesian inference for ill-posed problems via variational method. *J. Comput. Phys.*, 229(19):7317–7343, 2010.
- [29] H. Kadri, E. Duflos, P. Preus, S. Canu, A. Rakotomamonjy, and J. Audiffren. Operator-valued kernels for learning from functional response data. *J. Mach. Learn. Res.*, 17:1–54, 2016.
- [30] J. Kaipio and E. Somersalo. *Statistical and Computational Inverse Problems*. Springer-Verlag, New York, 2005.
- [31] D. A. Levin, Y. Peres, and E. L. Wilmer. *Markov Chains and Mixing Times*. American Mathematical Society, second edition, 2017.
- [32] Q. Liu and D. Wang. Stein variational gradient descent: A general purpose Bayesian inference algorithm. In *NeurIPS*, volume 29, 2016.
- [33] A. Logg, K. A. Mardal, and G. N. Wells. *Automated Solution of Differential Equations by the Finite Element Method*. Springer, United Kingdom, 2012.
- [34] Juan Carlos De los Reyes. *Numerical PDE-Constrained Optimization*. Springer, New York, 2015.
- [35] J. Lu, Y. Lu, and J. Nolen. Scaling limit of the Stein variational gradient descent: the mean field regime. *SIAM J. Math. Anal.*, 5(2):648–671, 2019.
- [36] A. G. D. G. Matthews. *Scalable Gaussian process inference using variational methods*. PhD thesis, University of Cambridge, 9 2016.
- [37] R. Nickl. Betnstein-von Mises theorem for statistical inverse problems I: Schrödinger equation. *J. Eur. Math. Soc.*, 22:2697–2750, 2020.
- [38] V. I. Paulsen and M. Raghupathi. *An Introduction to the Theory of Reproducing Kernel Hilbert Spaces*. Cambridge University Press, United Kingdom, 2016.
- [39] F. J. Pinski, G. Simpson, A. M. Stuart, and H. Weber. Algorithms for Kullback-Leibler approximation of probability measures in infinite dimensions. *SIAM J. Sci. Comput.*, 37(6):A2733–A2757, 2015.
- [40] F. J. Pinski, G. Simpson, A. M. Stuart, and H. Weber. Kullback-Leibler approximation for probability measures on infinite dimensional space. *SIAM J. Math. Anal.*, 47(6):4091–4122, 2015.
- [41] G. D. Prato. *An Introduction to Infinite-Dimensional Analysis*. Springer-Verlag, Berlin, 2006.
- [42] M. Reed and B. Simon. *Functional Analysis I: Methods of Modern Mathematical Physics*. Elsevier (Singapore) Pte Ltd, revised and enlarged edition, 2003.
- [43] A. Spantini, A. Solonen, T. Cui, J. Martin, L. Tenorio, and Y. Marzouk. Optimal low-rank approximations of Bayesian linear inverse problems. *SIAM J. Sci. Comput.*, 37(6):A2451–A2487, 2015.
- [44] A. M. Stuart. Inverse problems: A Bayesian perspective. *Acta Numer.*, 19:451–559, 2010.
- [45] S. Sun, G. Zhang, J. Shi, and R. Grosse. Functional variational Bayesian neural networks. In *ICLR*, 2019.
- [46] A. Tarantola. *Inverse Problem Theory and Methods for Model Parameter Estimation*. SIAM, United States, 2005.
- [47] A. Tarantola and B Valette. Inverse problems = quset for information. *J. Geophys.*, 50(1):159–170, 1982.
- [48] D. Wang, Z. Tang, C. Bajaj, and Q. Liu. Stein variational gradient descent with matrix-valued kernels. In *NeurIPS*, volume 33, 2019.
- [49] K. Wang, T. Bui-Thanh, and O. Ghattas. A randomized maximum a posteriori method for posterior sampling of high dimensional nonlinear Bayesian inverse problems. *SIAM J. Sci. Comput.*, 40(1):A142–A171, 2018.

- [50] Z. Wang, T. Ren, J. Zhu, and B. Zhang. Function space particle optimization for Bayesian neural networks. In *ICLR*, 2019.
- [51] C. Zhang, J. Butepage, H. Kjellstrom, and S. Mandt. Advances in variational inference. *IEEE T. Pattern Anal.*, 41(8):2008–2026, 2018.
- [52] Q. Zhao, D. Meng, Z. Xu, W. Zuo, and Y. Yan. l_1 -norm low-rank matrix factorization by variational Bayesian method. *IEEE T. Neur. Net. Lear.*, 26(4):825–839, 2015.
- [53] Q. Zhou, T. Yu, X. Zhang, and J. Li. Bayesian inference and uncertainty quantification for medical image reconstruction with poisson data. *SIAM J. Imaging Sci.*, 13(1):29–52, 2020.

SCHOOL OF MATHEMATICS AND STATISTICS, XI'AN JIAOTONG UNIVERSITY, XI'AN, 710049, CHINA

Email address: jjx323@xjtu.edu.cn

SCHOOL OF MATHEMATICS AND STATISTICS, XI'AN JIAOTONG UNIVERSITY, XI'AN 710049, CHINA

Email address: dymeng@mail.xjtu.edu.cn